SUPPLEMENT TO
LCGC north america
solutions for separation scientists
Volume 37 Number s11 November 2019
www.chromatographyonline.com

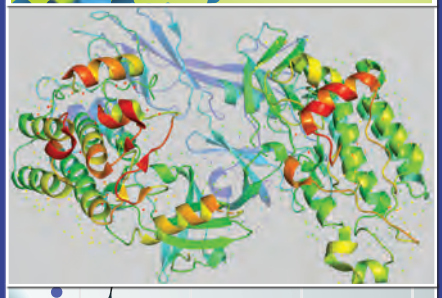

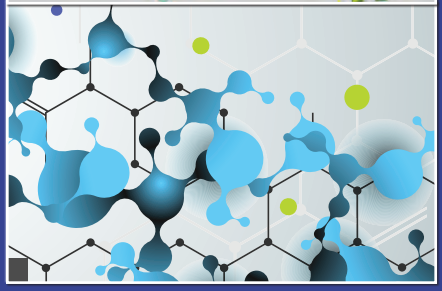

ADVANCES IN BIOPHARMACEUTICAL ANALYSIS

RESTEK | ADVANTAGE

See What It Can Do for You and Your Lab

- Technical Articles & Applications
- Videos & ChromaBLOGraphy
- FAQs & Troubleshooting
- Education & Instruction
- Online Tools & Calculators
- Product Selection Assistance

Sign up today to access Restek's years of chromatography knowledge at

www.restek.com/advantage

RESTEK Pure Chromatography

Agilent
Trusted Answers

Advancing Glycosciences. Together.

N-glycan characterization is essential to the development process because N-glycans on biotherapeutics can affect immunogenicity, pharmacokinetics, and pharmacodynamics.

Agilent is your single source for your glycan analysis workflow. With our addition of ProZyme products and services, you can now obtain everything you need to go from sample to answers. That includes sample preparation, enzymes, standards, columns, detection, analysis, and service.

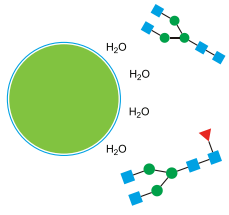

Let us help you push your protein analysis to new levels of performance.
www.agilent.com/chem/better-together

LCGC north america
solutions for separation scientists

MANUSCRIPTS: For manuscript preparation guidelines, see chromatographyonline.com/lcgc-author-guidelines, or call The Editor, (732) 596-0276. *LCGC* welcomes unsolicited articles, manuscripts, photographs, illustrations, and other materials but cannot be held responsible for their safekeeping or return. Every precaution is taken to ensure accuracy, but *LCGC* cannot accept responsibility for the accuracy of information supplied herein or for any opinion expressed.

SUBSCRIPTIONS: For subscription and circulation information: *LCGC*, P.O. Box 6168, Duluth, MN 55806-6168, or call (888) 527-7008 (7:00 a.m.–6:00 p.m. central time). International customers should call +1-218-740-6477. Delivery of *LCGC* outside the United States is 14 days after printing. For single and back issues, call (800) 598-6008 or (218) 740-6480. (*LCGC Europe* and *LCGC Asia Pacific* are available free of charge to users and specifiers of chromatographic equipment in Western Europe and Asia and Australia, respectively.)

CHANGE OF ADDRESS: Send change of address to *LCGC*, P.O. Box 6168, Duluth, MN 55806-6168; alternately, send change via e-mail to fulfill@hcl.com or go to the following URLs:
• Print: http://ubmsubs.ubm.com/?pubid=LCGC
• Digital: http://ubmsubs.ubm.com/?pubid=LCGC&V=DIGI
Allow four to six weeks for change. PUBLICATIONS MAIL AGREEMENT No. 40612608. Return all undeliverable Canadian addresses to: IMEX Global Solutions, P.O. Box 25542, London, ON, N6C 6B2, CANADA. Canadian GST number: R-124213133RT001.

C.A.S.T. DATA AND LIST INFORMATION: Contact Melissa Stillwell, tel. (218) 740-6831, e-mail MStillwell@mmhgroup.com.
REPRINTS: Contact Michael J. Tessalone, e-mail: MTessalone@mmhgroup.com
INTERNATIONAL LICENSING: Contact Kim Scaffidi, e-mail: kscaffidi@mjhassoc.com

CUSTOMER INQUIRIES: Customer inquiries can be forwarded directly to MJH Life Sciences, Attn: Subscriptions, 2 Clarke Drive, Suite 100, Cranbury, NJ 08512; e-mail: mmhinfo@mmhgroup.com

Alliance for Audited Media

50% Recycled Paper 10-20% Post Consumer Waste

485F US Highway One South,
Suite 210
Iselin, NJ 08830
(732) 596-0276
Fax: (732) 647-1235

PUBLISHING/SALES

Vice President/Group Publisher
Michael J. Tessalone
MTessalone@mmhgroup.com

Associate Publisher
Edward Fantuzzi
EFantuzzi@mmhgroup.com

Sales Manager
Brianne Molnar
BMolnar@mmhgroup.com

Senior Director, Digital Media
Michael Kushner
MKushner@mmhgroup.com

EDITORIAL

Editorial Director
Laura Bush
LBush@mmhgroup.com

Managing Editor
John Chasse
JChasse@mmhgroup.com

Senior Technical Editor
Jerome Workman
JWorkman@mmhgroup.com

Associate Editor
Cindy Delonas
CDelonas@mmhgroup.com

Art Director
Gwendolyn Salas
gsalas@mdmag.com

Graphic Designer
Courtney Soden
csoden@mjhassoc.com

CONTENT MARKETING

Custom Content Writer
Allissa Marrapodi
AMarrapodi@mmhgroup.com

Webcast Operations Manager
Kristen Moore
KMoore@mmhgroup.com

Project Manager
Vania Oliveira
VOliveira@mmhgroup.com

Digital Production Manager
Sabina Advani
SAdvani@mmhgroup.com

Managing Editor, Special Projects
Kaylynn Chiarello-Ebner
KEbner@mmhgroup.com

MARKETING/OPERATIONS

Marketing Manager
Anne Lavigne
ALavigne@mmhgroup.com

C.A.S.T. Data and List Information
Melissa Stillwell
MStillwell@mmhgroup.com

Reprints
Alexandra Rockenstein
ARockenstein@mmhgroup.com

Audience Development Manager
Jessica Stariha
JStariha@mmhgroup.com

CORPORATE

Chairman & Founder
Mike Hennessy Sr

Vice Chairman
Jack Lepping

President
Mike Hennessy Jr

Chief Strategy Officer & President, Agency Services
George Glatcz

Chief Financial Officer
Neil Glasser, CPA/CFE

Executive Vice President, Operations
Tom Tolvé

Senior Vice President, Content
Silas Inman

Senior Vice President, I.T. & Enterprise Systems
John Moricone

Senior Vice President, Development & Enterprise Systems
John Paul Uva

Senior Vice President, Audience Generation & Product Fulfillment
Joy Puzzo

Vice President, Human Resources & Administration
Shari Lundenberg

Vice President, Business Intelligence
Chris Hennessy

Vice President, Corporate Branding & B2B Marketing
Amy Erdman

Executive Creative Director, Creative Services
Jeff Brown

Advances in Biopharmaceutical Analysis

A supplement to LCGC North America

November 2019

Articles

Cover Images: ustas - stock.adobe.com | vectorfusionart - stock.adobe.com | Leonid - stock.adobe.com | sergunt - stock.adobe.com

FROM the GUEST EDITOR

Advancing Biopharmaceutical Analysis

Cinzia Stella *Senior Scientist, Genentech*

Over the past few years, complex and novel format biotherapeutics, such as fusion products, bispecific antibodies, protein–polymer conjugates, and coformulations have been increasingly populating the pipeline of many biotech companies. At the same time, the growing demand to reduce the time it takes to develop and bring new medicines to patients has shed light on the limitations of current analytical tools and standard technical development considerations with next-generation biologics. In this increasingly competitive landscape, analytical methods that can provide improvements in speed, resolving power, and overall separation efficiency are highly desirable and critical to ensure that sufficient product characterization is performed at each stage of development.

This special issue was assembled to showcase recent advances in the development of analytical workflows and characterization strategies that are currently used for product quality control (QC) testing, monitoring of undesired variants, and identification of critical quality attributes (CQAs). This issue also highlights key considerations to be taken into account throughout the development of novel and unique formats and is aimed to provide valuable insight into how to overcome challenges that might be associated with next-generation biotherapeutics. Some of the articles are the result of key collaborations between industry and academic leaders, highlighting the necessity of synergistic efforts for the development and implementation of novel analytical workflows and strategies.

Jennifer Rea and her coauthors provide an overview of the increased complexity of characterization and quality control by size-exclusion chromatography (SEC) of complex biotherapeutics compared to standard monoclonal antibody formats. SEC is typically used to separate and quantify product variants and to monitor in particular the level of aggregates, which often represent a safety concern. Examples of SEC analysis of bispecific, antibody–drug conjugate (ADC), and coformulated products are described, as well as unique considerations for achieving desired peak separation.

Further insight into technical considerations for a product-specific SEC method for QC is provided by Lu Dai and coauthors. To increase the half-life of a therapeutic protein, a complex multi-arm polyethylene glycol (PEG) scaffold was coupled to the protein as a means to increase the size and therefore the half-life of the product in the eye. In this case, given the major impact of size on the desired half-life, the challenge was to develop a suitable SEC method to be used for QC for the separation and quantification of the product size variants, covering a much wider range (from 50 to >1000 kDa) than for standard monoclonal antibodies (mAbs).

In a demonstration of a growing trend in biotherapeutics to design molecules with a high degree of valency, Whitney Shatz and coauthors describe an alternative approach to polymer-based scaffolds. Multivalent, self-assembling scaffolds such as ferritin can be effectively used for such purpose in drug delivery. This study, like the others presented in this special issue, provides valuable insight into analytical methods that are needed to support both optimization of the manufacturing process and QC of the final product. In this work, SEC in-line with a multi-angle light scattering detector (MALS) and quasi-elastic light scattering detector (QELS) were crucial to assess the molecular size under native conditions and inform the optimization of the conjugation process.

Ming Lei and Tao Chen offer an overview of considerations and recent developments for the quantification of product-related variants of bispecific antibodies, another approach to achieve simultaneous binding to two targets with high specificity. This article highlights the crucial need of having an analytical assay that can detect the presence of the undesired homodimer variant, both during the development of the manufacturing process to facilitate the removal and during final product QC. Given that the undesired homodimer has very similar physico-chemical properties to the desired heterodimer, the limits of standard analytical methods (such as SEC), as described by Rea et al., become apparent in this situation. An alternate approach is therefore provided by Lei and Chen, where the bispecific product is reduced to its subunits using hinge-specific enzymes, prior to chromatographic separation. The authors also presented the method qualification strategy and results of an ion-exchange chromatography (IEX)-based homodimer quantitation method in anticipation of a charge patch on a bispecific antibody.

Another critical analytical method for the characterization of biotherapeutics is peptide mapping by liquid chromatography–tandem mass spectrometry (LC-MS/MS). This tool is routinely used for the identification and quantification of post-translational modifications (PTMs) such as oxidation, deamidation, and isomerization. Given that some PTMs can be CQAs, it is crucial to provide reproducible and accurate quantitative information when using this method. Michael Mølhøj and his coauthors share their findings on how oxidative artifacts can affect the quantitation of inherent product heterogeneities and therefore generate misleading information. They offer a valuable approach to mitigate the effect of on-column oxidation when performing peptide mapping.

Julien Camperi and Arthur Schick offer an overview of how multidimensional on-line peptide mapping can streamline the post-labeling workflow of hydroxyl radical footprinting–mass spectrometry (HRF-MS) analysis. This work highlights how automated on-line peptide mapping can significantly reduce sample handling and operator time compared to standard off-line procedures.

Overall, this special issue highlights challenges and opportunities for the characterization of complex and unique format molecules entering the pipeline and describes examples of analytical workflows and control strategies when standard QC platform methods and approaches are not applicable. The analytical workflows and strategies are evolving along with biotherapeutic pipelines to enable faster development of promising and novel medicines to fulfill unmet medical needs.

If your standards and your samples are the same size, they must be the same mass, right?

With DAWN you can determine absolute molecular weights and sizes without using reference standards made in someone else's lab.

That's the problem with calibration-based measuring techniques. You don't know—you can only assume. Which is why every major pharmaceutical and biotechnology company, as well as most federal regulatory agencies are switching from relative methods to Wyatt Technology's absolute measurements. Our DAWN® multi-angle light scattering (MALS) instruments allow you to determine absolute molecular weights and sizes without relying on so-called standards, or measurements made in someone else's lab. Wyatt instruments measure all of the quantities required for determining absolute molar masses directly.

Learn how to end you dependence on reference standards forever at wyatt.com/NoRef

WYATT TECHNOLOGY
wyatt.com

Monitoring of On-column Methionine Oxidation as Part of a System Suitability Test During UHPLC–MS/MS Peptide Mapping

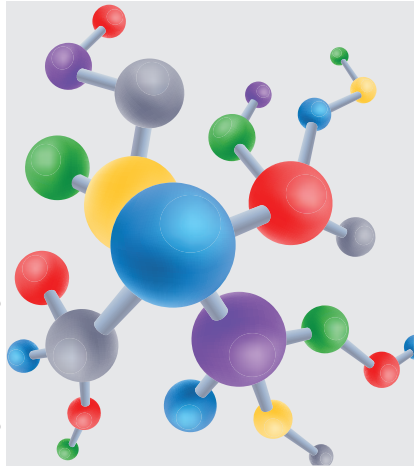

Image credit: Designincolor/stock.adobe.com

Peptide mapping by liquid chromatography–tandem mass spectrometry (LC–MS/MS) is an essential analytical tool for the characterization of biotherapeutics, such as for the identification and quantification of post-translational modifications, including oxidation. Therefore, is it crucial that the LC–MS system is performing under optimal conditions, ensuring reproducible and accurate quantitative information. A system suitability test is usually performed prior to sample analysis to confirm that the sample preparation and instrument performance are adequate and running as expected. Induced in-source oxidation is a known phenomenon associated with the electrospray process, and can be discriminated from relevant sample oxidation. On-column methionine oxidation can also take place during LC–MS/MS peptide mapping analysis of antibody-based biotherapeutics over long-term column use. This article describes how the monitoring of on-column methionine oxidation as part of system suitability testing can be used to control unintended on-column methionine oxidation of biotherapeutics. This approach minimizes the risk of measuring oxidative artifacts, and helps generate high quality data to provide reliable quantitative information about product-related heterogeneities.

Björn Mautz*, Vincent Larraillet*, Maximiliane König, and Michael Mølhøj

** Both authors contributed equally to this work.*

Peptide mapping by ultrahigh-pressure liquid chromatography–tandem mass spectrometry (UHPLC–MS/MS) is extensively used for various purposes, such as identity testing, disulfide bond analysis, host cell protein analysis, sequence variant analysis, assessment of potential critical quality attributes, and multiple-attribute methodology (MAM) workflows for biotherapeutics, including the evaluation of post-translation modifications (PTMs). PTMs occur at distinct amino acid side chains or peptide linkages, and are added shortly after translation is completed, after folding during passage through the Golgi apparatus, upon bioprocessing, storage, stress, or after administration. In therapeutic proteins, PTMs are especially critical if they negatively influence drug potency or safety. It is therefore essential to ensure reproducibility in the manufacturing process of therapeutic proteins so that there is no significant difference in the effective dose, and to prevent unexpected side effects. Consequently, PTMs need to be monitored and controlled to demonstrate batch consistency and comparability of manufactured clinical material. It is essential that the sample preparation method, the liquid chromatography system, and the mass spectrometer are performing optimally to ensure reliable data. For example, suitable endoproteolytic digestion methods at mildly acidic conditions (pH 6.0) have been developed to keep to a minimum artificial deamidation and succinimide formation (1–2).

Oxidation is a source of protein variability and one of the major degradation pathways for protein ther-

Table I: Relative abundance of the six most oxidized bsAb1 tryptic peptides using the aged reversed-phase chromatography column (~1500 column runs) and the expected levels of oxidation based on historical data.

Peptide[a]	Molecular Localization	Relative Abundance of Oxidation (%)[b]	
		Amount Measured on Aged Column[c]	Amount Based on Historical Data[d]
DTLMISR	CH_2 domain	30	2
QAPGQGLEWMGR	VH framework region	15	0.1
XXXMXXXX[e]	LC-CDR1	13	0.8
SQVVLTMTNMDPVDTATYYCAR	VH framework region	10	0.8
$SLSLSPG(G_4S)_4X_{17}$	CH_3-Linker-Fusion	8	0.1
VTITADTSTSTAYMELSSLR	VH framework region	3	0.3

(a) Oxidized peptide as determined by LC–MS. (b) Evaluation by extracted ion current chromatograms. (c) Sum of in-sample, on-column and in-source oxidations. (d) In-sample oxidation only (no on-column oxidation detected). (e) Undisclosed amino acid sequence.

apeutics in vitro and in vivo. The sulfur-containing cysteine (unpaired) and methionine residues are particularly susceptible to oxidation (3), and are often monitored during formulation development, batch characterization, and long-term stability studies. Protein oxidation can lead to diverse functional consequences, such as lower activity or potency, increased susceptibility to aggregation, and altered immunogenicity (4–10). Methionine residues are readily oxidized to methionine sulfoxide (MetO) *S*- and *R*-diastereomers by many reactive species adding oxygen to the sulfur atom (11–13), and the reaction is essentially pH independent (14). Given that MetO is more hydrophilic relative to methionine, it will elute earlier on a reversed-phase column (15). The level of sample oxidation can be easily quantified by comparing the peak area of the MetO with the methionine peak. In addition to the sample oxidation, a redox reaction in the electrospray ionization (ESI) source can also occur, causing artificial in-source oxidations (16–17). Usually, in-source oxidation can be easily detected based on the identical elution profile of modified and unmodified peptides, allowing in-source oxidation to easily be discriminated from in-sample oxidation (15). MetO can be further oxidized to methionine sulfone ($MetO_2$). Other commonly oxidized residues include tryptophan and histidine (18–19).

A system suitability test (SST) is typically part of an analytical method to confirm that the sample preparation and the entire instrument performance are adequate to ensure reproducible and accurate results (20-21). Lack of an adequate SST may generate poor quality data and misleading information. Here, we report the observation of unexpected on-column methionine oxidation during LC–MS/MS peptide mapping analysis and its impact on the SST sample. This study shows how the quantitative evaluation of methionine oxidation was found to be susceptible to significant variability over long-term reversed-phase column use, and how a suitable SST may mitigate the effects of on-column oxidation.

Figure 1: Extracted ion current chromatograms of unmodified (black) and oxidized (red) bsAb1 tryptic peptides (amino acid sequence indicated, see also Table I) using an aged (~1500 column runs) (a-c and g-i) and a new (d-f and j-l) reversed-phase C18 column. (c and f) The amino acid sequence of the LC-CDR1 covering peptide indicated by XXXMXXXX is undisclosed. (j) Two in-sample oxidation peaks observed likely due to the peptide (amino acid sequence: SQVVLTMTNMDPVDTATYYCAR) containing two methionine residues. In-Sa, in-sample oxidation; On-Co., on-column oxidation; In-So., in-source oxidation; URP, unrelated peptide.

Table II. System suitability acceptance criteria for the system suitability test sample

Description					Aged Column[a]	New Column
I	mAb2 sequence coverage ≥70% of 20 unique peptides[b]				81	86
II	Recovery rate for mAb2 peptides: ≥15 of 20 unique findable peptides				18/20	19/20
III	Consistent retention times between relevant SST sample runs for three mAb2 tryptic peptides					
	Peptide	Mass (Da)	Ion extraction (*m/z*)	Approximate retention time (min)[d]	Consistent retention time	
	A	706.365	354.190 ±0.003	~13	Passed	Passed
	B	1880.996	941.505 ±0.008	~48	Passed	Passed
	C[c]	4656.031	1165.015 ±0.009	~69	Passed	Passed

System suitability test sample is mAb1 spiked with 0.5% (w/w) mAb2. (a) ~1500 column runs. (b) Covering complementarity-determining regions and the kappa light chain. (c) Cys alkylated using ^{13}C iodoacetic acid. (d) Retention times may vary slightly between different batches of the reversed-phase column.

Materials and Methods

Enzymes and Antibodies

Trypsin was purchased from Promega. The bispecific antibody (bsAb1) sample was stably expressed in Chinese hamster ovary (CHO) cells, and purified from a platform fed batch fermentation. The SST sample consisting of a monoclonal antibody (mAb1, lambda light chain) spiked with 0.5% (*w/w*) of a second monoclonal antibody (mAb2, kappa light chain) was stored as ready-to-use 25 µL aliquots (concentration is 10 mg/mL) at –80 °C.

Tryptic Digests

Both bsAb1 and the SST sample were denatured and reduced in 0.3 M tris-HCl pH 8, 6 M guanidine-HCl and 20 mM dithiothreitol (DTT) at 37 °C for 1 h, and alkylated by adding 40 mM iodoacetic acid (^{13}C: 99%) (Sigma-Aldrich) at room temperature and in the dark for 15 min. Excess iodoacetic acid was inactivated by adding DTT to a total of 40 mM. The alkylated proteins were buffer exchanged using NAP5 gel filtration columns (GE Healthcare), and digested with trypsin in 50 mM tris-HCl, pH 7.5 at 37° C for 16 h. The reactions were stopped by adding formic acid to 0.4% (*v/v*). Digested samples were stored at –80 °C until analysis.

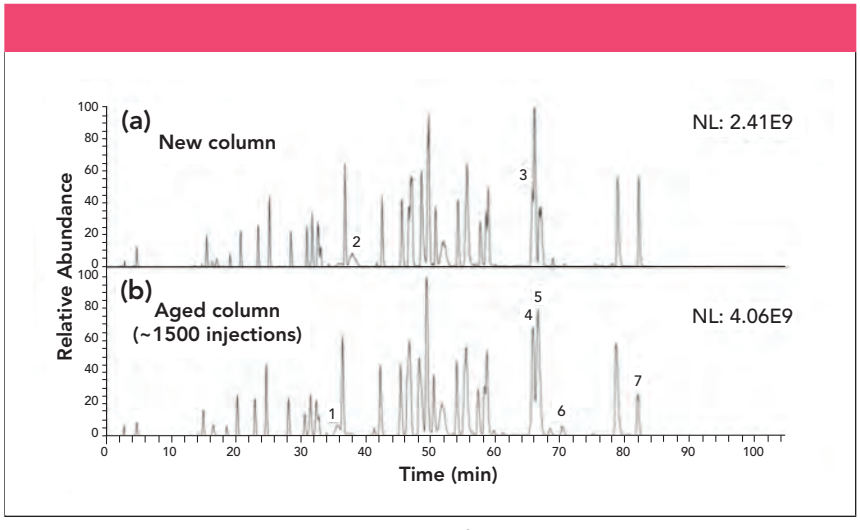

Figure 2: Total ion current chromatograms of the tryptic digested system suitability test sample (surrogate mAb1 spiked with 0.5% (*w/w*) mAb2), using (a) a new column (two injections), and (b) an aged reversed-phase C18 column. The apparent differences (numbered peaks) were identified as the following mAb1 peptides: 1) heavy chain AA349-359 without missed cleavages, 2) heavy chain AA349-364 with one missed cleavage, 3) heavy chain AA223-252 with two missed cleavages, 4) heavy chain AA306-321 without missed cleavages, 5) heavy chain AA227-252 with one missed cleavage (increased levels with the aged column) and heavy chain AA20-38 without missed cleavages (similar levels with both columns), 6) unassigned peptides likely containing missed cleavages, and 7) light chain AA131-150 without missed cleavages. NL, normalized intensity level.

UHPLC–MS/MS Analysis

The tryptic digests were analyzed by UHPLC–MS/MS using a Vanquish UHPLC system (Thermo Fisher Scientific) and an Orbitrap Fusion Lumosmass spectrometer (Thermo Fisher Scientific). For each analyzed sample, 2.5 µg of digested protein were injected onto the UHPLC system. Chromatographic separation was performed by reversed-phase LC on a BEH300 C18 column (1 mm x 150 mm, 1.7-µm) (Waters) using mobile phase A and B containing 0.1% formic acid (*v/v*) in UHPLC grade water and acetonitrile, respectively (Optima LC–MS quality; Fisher Chemical). A 60 µL/min flow rate, a 50 °C column temperature, and the following gradient were used: 1% mobile phase B (0–3 min), 1% to 40% mobile phase B (3–93 min), 40% to 99% mobile phase B (93-94 min), 99% mobile phase B (94–96 min), 99% to 1% mobile phase B (96–97 min), and 1% mobile phase B (97–105 min). Two blank injections of mobile phase A, using a 50 min gradient up to 99% mobile phase B, were performed between sample injections to reduce carry-over. The SST sample was run at the beginning and the end of each sequence to ensure suitability of the system for the entire sequence. The column was stored in 80% (*v/v*) acetonitrile after usage.

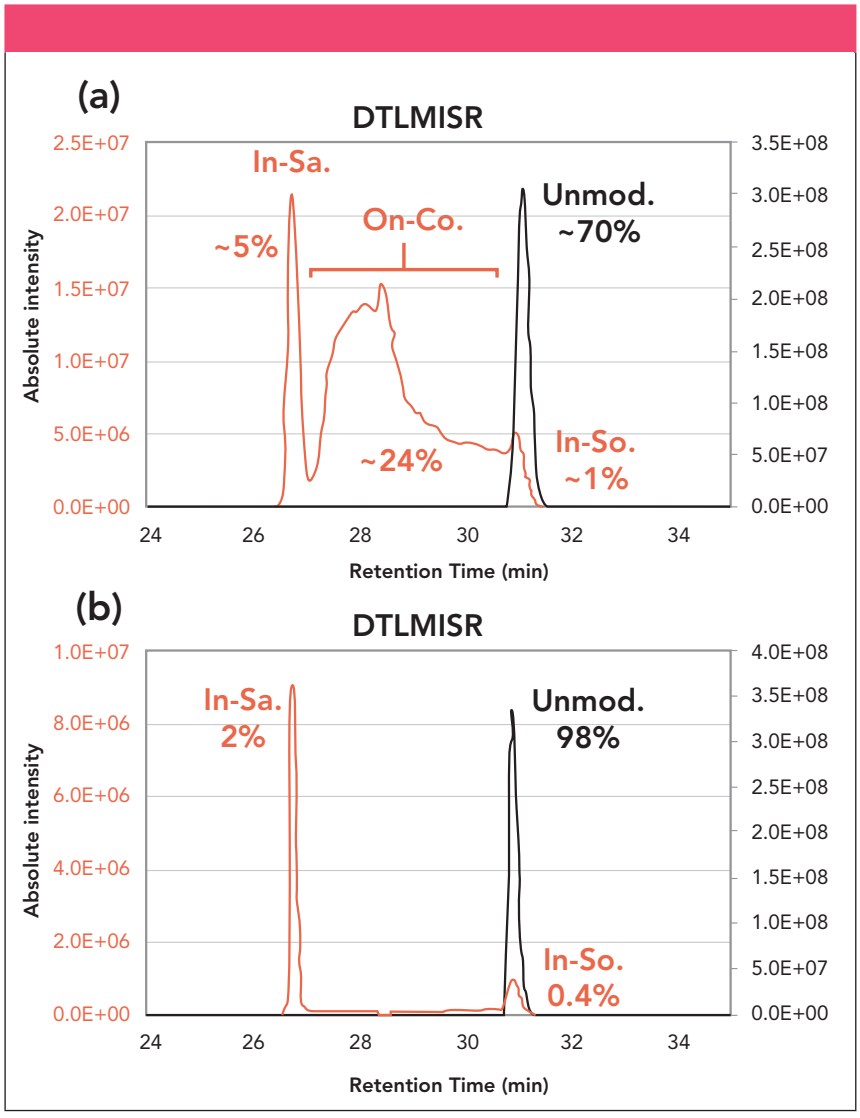

Figure 3: Extracted ion current chromatograms of the single protonated, unmodified (black) and oxidized (red) system suitability test sample peptide DTLMISR using (a) the aged (~1500 column runs) reversed-phase C18 column, and (b) a new reversed-phase C18 column. For the aged column, approximate relative numbers are indicated as the oxidized peptides were not baseline separated. In-Sa, in-sample oxidation; On-Co., on-column oxidation; In-So., in-source oxidation.

MS/MS Data Acquisition

High-resolution MS/MS spectra were acquired with the orbital trap mass analyzer, and detection of higher-energy collisional dissociation (HCD) fragment ion spectra with dynamic exclusion enabled (repeat count of 1, exclusion duration of 15 s [±10 ppm]). The orbital trap Fusion Lumos was used in the data-dependent mode. HCD essential settings were: full MS (automatic gain control (AGC): 4 x 105, resolution: 1.2 x 105, *m/z* range: 300-2000, maximum injection time: 50 ms), MS/MS OT (AGC: 5.0 x 104, maximum injection time: 500 ms, isolation window: 2), orbital trap resolution was 15 x 103, MS/MS IT (AGC: 1.0 x 104, maximum injection time: 100 ms, isolation window: 2), normalized collision energy was set to 28%.

Data Processing

Analysis of the MS/MS data was performed using the Byos/Byologic v3.3 software (Protein Metrics). Manual data interpretation and quantification was performed using the Xcalibur Qual Browser v.4.0 (Thermo Fisher Scientific). Extracted ion current chromatograms were generated with the most intense isotope masses.

Results and Discussion

During the peptide mapping analysis of the unstressed bsAb1 sample, unexpected high levels of oxidations were observed using a qualified UHPLC–MS/MS based method and a reversed-phase column that at the time of this analysis had been used for ~1500 column runs. The observed oxidation affected several methionine-containing tryptic peptides from complementarity-determining, variable framework, and the fragment crystallizable (Fc) regions. The six mostly oxidized peptides are listed in Table I. Relative oxidation levels ranging from 0.1% to 2% were expected for all oxidized peptides based on historical data. However, using the aged column, the oxidation levels of the six peptides ranged between 3% and 30% (Table I). When the same samples were reanalyzed on a new column under the same conditions, the observed oxidation levels were comparable to the expected values (historical data) for all oxidized peptides (Table I).

A closer inspection of the extracted ion current (EIC) chromatograms of the oxidized peptides using the aged column demonstrated that the chromatograms exhibited unusual elution profiles. Using the aged column, the oxidized peptides eluted continuously over ~5–9 min, giving rise to distorted and broadened peaks (Figure 1a–c, 1g–i). Using a new column, the oxidized peptides eluted as distinctive peaks (Figure 1d–f, 1j–l). Given that this kind of continuous elution profile for oxidized peptides (on the aged column) had not been observed previously, the initial hypothesis was that either the eluents or the chromatography column could be the potential root cause. Given that the same mobile phases were used with both the aged and new column runs, the broadened oxidation peaks could only be explained by an on-column oxidation reaction taking place on the stationary phase surface of the UHPLC column during the peptides' elution. Using the new column, the in-sample and in-source induced oxidized peptides were baseline separated and

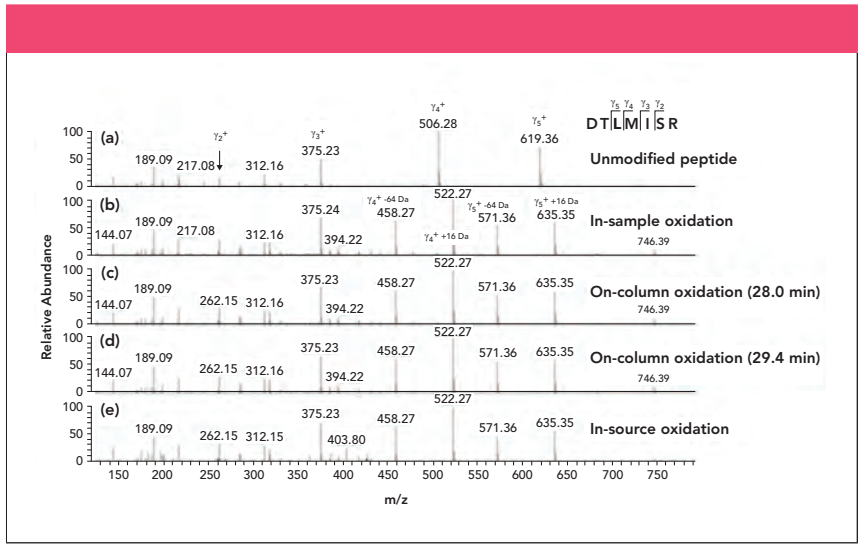

Figure 4: Orbital trap MS/MS spectra obtained by higher-energy collisional dissociation of the single protonated and (a) unmodified DTLMISR peptide, (b) in-sample oxidized, (c) on-column oxidized (28.0 min), (d) on-column oxidized (29.4 min), and (e) in-source oxidized DTLMISR peptides of the system suitability test sample using the aged column (see Figure 3a). Mass differences between the y4$^+$ (*m/z* 506.28) and y5$^+$ (*m/z* 619.36) fragment ions of the unmodified DTLMISR peptide, and the y4$^+$ (*m/z* 522.27) and y5$^+$ (*m/z* 635.35) fragments ions of the modified peptides demonstrate the methionine residues to be modified by +16 Da. In addition, the presence of neutral losses of 64 Da corresponding to methane sulfenic acid (CH_3SOH) of the y4$^+$ and y5$^+$ fragment ions resulting in y4$^+$-64 Da (*m/z* 458.27) and y5$^+$-64 Da (*m/z* 571.36) further prove the modified peptides to be methionine oxidized.

typical profiles were observed in the course of the chromatographic separation (Figure 1d–f, 1j–l). In-sample oxidized peptides had earlier retention times than the in-source oxidized peptides due to the interaction with the reversed-phase column by the in-sample oxidized peptides. On-column oxidation was defined by oxidation that was only observed with the aged reversed-phase column. No increased methionine di-oxidation or tryptophan oxidation were observed in any bsAb1 peptides.

The unusually high levels of peptide oxidation using the aged column compelled us have a deeper look at the SST data, and the system performance in general. The SST selected for this study was a sample consisting of a monoclonal antibody mAb1 spiked with 0.5% (*w/w*) of a second monoclonal antibody mAb2. The SST sample was digested with the same procedure and at the same time as the other samples, and then run at the beginning and at the end of each sequence. The sample preparation and LC–MS system are considered suitable if three acceptance criteria are met, namely 1) the mAb2 sequence coverage (positive identification by MS/MS of ≥70% of 20 unique peptides covering the complementarity-determining regions and the kappa light chain), 2) the mAb2 peptide recovery rate (≥15 of the 20 unique peptides), and 3) consistent retention times within acceptable ranges for three mAb2 tryptic peptides (A, B, and C) for all SST samples within a sequence. Further evaluations included visual inspections of the total ion current (TIC) chromatograms of the blank and the sample runs.

In the present study, the SST sample was used on both the aged and the new columns. Although the mAb2 sequence coverage and peptide recovery rate of the 20 unique peptides were slightly reduced on the aged column compared to the new column, all three SST criteria were met using the aged column (Table II). However, a visual inspection of the TIC chromatograms revealed some differences between the new and the aged columns in the intensities of a few peaks (peaks 1–7, Figure 2), which were attributed to the presence or absence of missed trypsin cleavages (Figure 2). These data suggested that the differences between the aged and new column TIC profiles could also be related to the sample preparation (tryptic digest efficiency) in addition to the column aging.

Using the aged column, the peptide with the amino acid sequence DTLMISR was determined to be the most oxidized amongst the tryptic bsAb1 peptides (Table I). This pep-

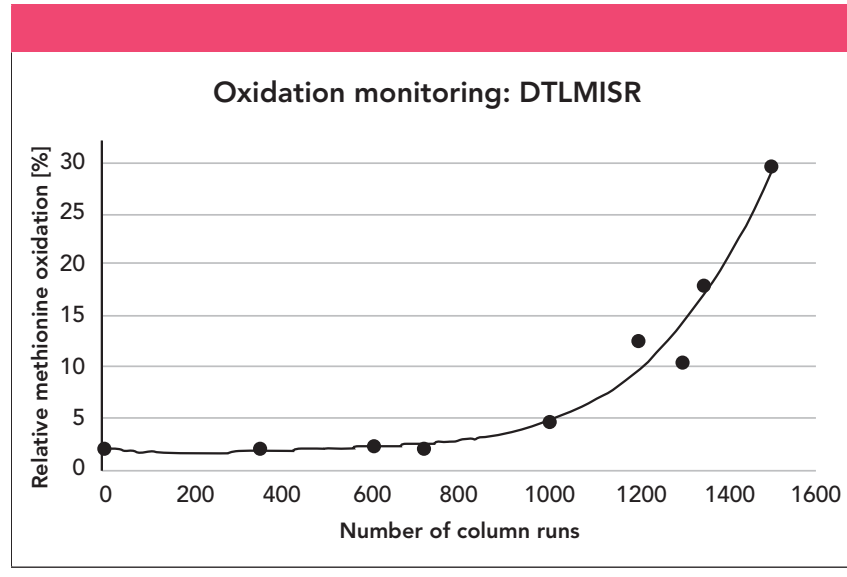

Figure 5: Relative abundance of methionine oxidized DTLMISR peptide (sum of in-sample, on-column, and in-source oxidation) of the SST sample dependent on the number of reversed-phase column runs as determined by extracted ion current chromatograms. With increasing on-column oxidation, the in-sample, on-column, and in-source oxidized peptides were not base-line separated.

tide is common to the Fc region of all four subclasses of immunoglobulins (IgG1-4), and the methionine residue Met252 is known to be susceptible to oxidation in intact immunoglobulins (22–23). Similarly to the bsAb1 sample, the DTLMISR peptide of the SST sample was also determined to be the most oxidized with approximately 5% in-sample, 24% on-column, and 1% in-source oxidation on the aged column (Figure 3a). As the oxidized DTLMISR peptides were not baseline separated, a more exact quantification is difficult with the aged column. Besides, the in-sample and in-source oxidation peaks may contain some on-column oxidation. Using the new column, the same peptide was determined to be 2% in-sample and 0.4% in-source oxidized, and no on-column oxidation was detected (Figure 3b). An inspection of the MS/MS spectra of the SST sample using the aged column confirmed that the in-sample (elution time: 26.7 min), on-column (at 28.0 min and 29.4 min), and in-source (31.0 min) modified peptides (Figure 3a) all contained an oxidized methionine residue in the same position (DTLMISR) (Figure 4).

Following these observations, we investigated the correlation between the on-column methionine oxidation and the long-term column usage. By looking at the historical SST data generated on the aged column, the relative abundance of the methionine oxidized DTLMISR peptide was found to be dependent on the number of column runs (Figure 5). Until about 700–800 columns runs, the level of in-sample oxidation was constant at ~2% relative abundance. After ~1500 column runs, the oxidation of the DTLMISR peptide gradually increased to a total oxidation level of 30% (sum of in-sample, on-column, and in-source oxidation). Following these observations, monitoring of MetO has been included as part of the SST while quantifying protein oxidation by peptide mapping. This control minimizes the risk of oxidative artifacts and helps generate high quality data to provide reliable quantitative information on protein oxidation.

On-column oxidation occurring on LC columns has been previously reported (24–25), and, in those studies, it was concluded that the oxidation reaction was due to metal catalysis of the column frits caused by trace levels of residual metal ions, most likely introduced from any surface in contact with the sample (25). A chelating agent ethylenediaminetetraacetic acid (EDTA) may be helpful to prevent or minimize the on-column oxidations and consequently extend the column lifetime. Also, the addition of antioxidants like methionine to the eluents could help protect the methionine containing peptides from oxidative damage.

Conclusions

In this study, we describe the impact of long-term column usage on the artificial increase of methionine oxidation during LC–MS/MS peptide mapping. Qualitative evidence for the on-column oxidation reaction was obtained by examination of the EIC chromatograms. The extent of the on-column oxidation significantly increased beyond 700–800 column runs, and the likely root cause is the presence of trace level metal ions on the chromatographic column. As a practical measure, we now visually/qualitatively monitor the level of on-column methionine oxidation of the SST sample tryptic peptide DTLMISR, which was oxidized to the highest level in this study.

Acknowledgments

The authors wish to thank the mass spectrometry team at Roche Innovation Center Munich for their support. We thank Cinzia Stella (Genentech) for carefully proofreading our manuscript.

References

(1) H.Z. Huang, A. Nichols, and D. Lu, *Anal. Chem.* **81**(4), 1686–1692 (2009).

(2) K. Diepold, K. Bomans, M. Wiedmann, B. Zimmermann, A. Petzold, T. Schlothauer, R. Mueller, B. Moritz, J.O. Stracke, M. Mølhøj, D. Reusch, and P. Bulau, *PLoS One* **7**(1), e30295 (2012).

(3) G. Xu and M.R. Chance, *Anal. Chem.* **77**(14), 4549–4555 (2005).

(4) L. Fucci, C.N. Oliver, M.J. Coon, and E.R. Stadtman, *Proc Natl Acad Sci USA* **80**(6), 1521–1525 (1983).

(5) J.L. Liu, K.V. Lu, T. Eris, V. Katta, K.R. Westcott, L.O. Narhi, and H.S. Lu, *Pharm Res.* **15**(4), 632–640 (1998).

(6) E.R. Stadtman, *Free Radic. Biol. Med.* **9**(4), 315–325 (1990).

(7) E. Shacter, J.A. Williams, and R.L. Levine, *Free Radic. Biol. Med.* **18**(4), 815–821 (1995).

(8) E. Shacter, *Drug Metab. Rev.* **32**(3-4), 307–326 (2000).

(9) S. Hermeling, D.J.A. Crommelin, H. Schellekens, and W. Jiskoot, *Pharm Res.* **21**(6), 897–903 (2004).

(10) D. Liu, D. Ren, H. Huang, J. Dankberg, R. Rosenfeld, M.J. Cocco, L. Li, D.N. Brems, and R.L. Remmele, Jr., *Biochemistry* **47**(18), 5088–5100 (2008)

(11) T.F. Lavine, *J .Bio.l Chem.* **169**(3), 477–491 (1947).

(12) W.E. Savige and A. Fontana, *Methods Enzymol.* **47,** 453–459 (1977)

(13) W. Vogt, *Free Radic. Biol. Med.* **18**(1), 93–105 (1995).

(14) A.V. Peskin and C.C. Winterbourn, *Free Radic. Biol. Med.* **30**(5), 572–579 (2001).

(15) Y. W. Lao, M. Gungormusler-Yilmaz, S. Shuvo, T. Verbeke, V. Spicer, and O.V. Krokhin, *J. Proteomics* **125**, 131–139 (2015).

(16) B.L. Boys, M.C. Kuprowski, J. Noël, and L. Konermann, *Anal. Chem.* **81**(10), 4027–4034 (2009).

(17) R. D. Espy, M. Wleklinski, X. Yan, and R.G. Cooks, *Trends Anal. Chem.* **57,** 135–146 (2014).

(18) E.R. Stadtman, *Annu. Rev. Biochem.* **62,** 797–821 (1993)

(19) J.O. Konz, J. King, and C.L. Cooney, *Biotechnol. Prog.* **14**(3), 393–409 (1998).

(20) J.C. Wahlich and G.P. Carr. *J. Pharm. Biomed. Anal.* **8**(8-12), 619–623 (1990).

(21) J.W. Dolan, *LCGC Europe* **17**(6), 328–332 (2004).

(22) W. Burkitt, P. Domann, and G. O'Connor, *Protein Sci.* **19**(4), 826–835 (2010)

(23) J. Stracke, T. Emrich, P. Rueger, T. Schlothauer, L. Kling, A. Knaupp, H. Hertenberger, A. Wolfert, C. Spick, W. Lau, G. Drabner, U. Reiff, H. Koll, and A. Papadimitriou, *MAbs* **6**(5), 1229–1242 (2014).

(24) J.-X. Huang, J.B. Stuart, W.R. Melaner, and C. Horváth, *J. Chromatogr.* **316,** 151–161 (1984).

(25) C. Tang, J. Tan, J. Jin, S. Xi, H. Li, Q. Xie, and X. Peng, *Rapid Commun. Mass Spectrom.* **29**(20), 1863–1873 (2015).

Björn Mautz, Vincent Larraillet, Maximiliane König, and Michael Mølhøj are with the Large Molecule Research group in Roche Pharma Research and Early Development (pRED) at the Roche Innovation Center Munich, in Penzberg, Germany. Direct correspondence to: michael.molhoj@roche.com

Considerations and Advances in Developing Analytical Assays for Measuring Product-Related Variants in Bispecific Antibodies

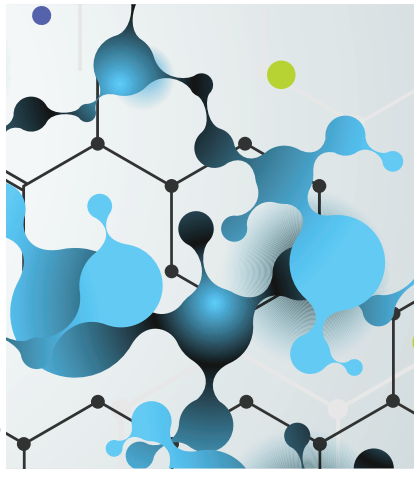

Image credit: Leonid/stock.adobe.com

Bispecific antibodies open new opportunities in drug development and have become a desirable drug format in cancer immunotherapy. In this type of application, one arm of the bispecific antibody binds to a cancer-specific receptor, while the other arm binds to a T-cell specific receptor to induce cancer cell elimination. Because up to four different polypeptide chains are involved in the assembly of a full-length bispecific antibody, many strategies have been developed to maximize the yield of the desired product (heterodimer) and facilitate the removal of undesired variants, such as homodimers. The successful adaptation of each strategy requires the development of suitable analytical methods to detect and measure the levels of undesired variants. Because the physicochemical properties of the undesired variants can be very similar to those of the desired heterodimer, it is paramount to magnify the minor differences as part of method development. In addition, given that the facilitation of heterodimerization of bispecific antibodies often relies on specific mutations that may impact the physicochemical properties, additional method assessments may need to be considered to ensure their suitability, such as interference from desired product to undesired variants. In the first half of this article, a summary of the common strategies employed in the production of full-length bispecific antibodies is provided. Then two case studies are presented in the second half. In the first case study, the proof-of-concept results are shared for a novel analytical method for variant detection using hinge-specific proteases that cleave at defined sites above or below the disulfide bonds in the hinge region. In the second case study, the method qualification experiments are described for a homodimer quantitation method to address the potential charge–charge interaction between a homodimer and the desired heterodimer.

Ming Lei and Tao Chen

Bispecific molecules are molecules that can simultaneously bind to two targets with high specificity, and are now emerging as a growing class of cancer immunotherapies (1–3). They include full-length bispecific antibodies, Fc-less bispecific molecules, fusion proteins, and many other forms of engineered proteins (3). Bispecific antibodies have many desired properties that are made possible by simultaneous binding to two targets. This class of therapeutic proteins (4) has been applied or is being tested for a wide range of applications, such as 1) inducing cancer cell killing by T-cells or natural killer (NK) cells through simultaneous binding to a cancer cell surface marker and an immune cell surface antigen, such as CD3; 2) activating or inhibiting a specific cellular pathway through simul-

Spin Me Right Round...

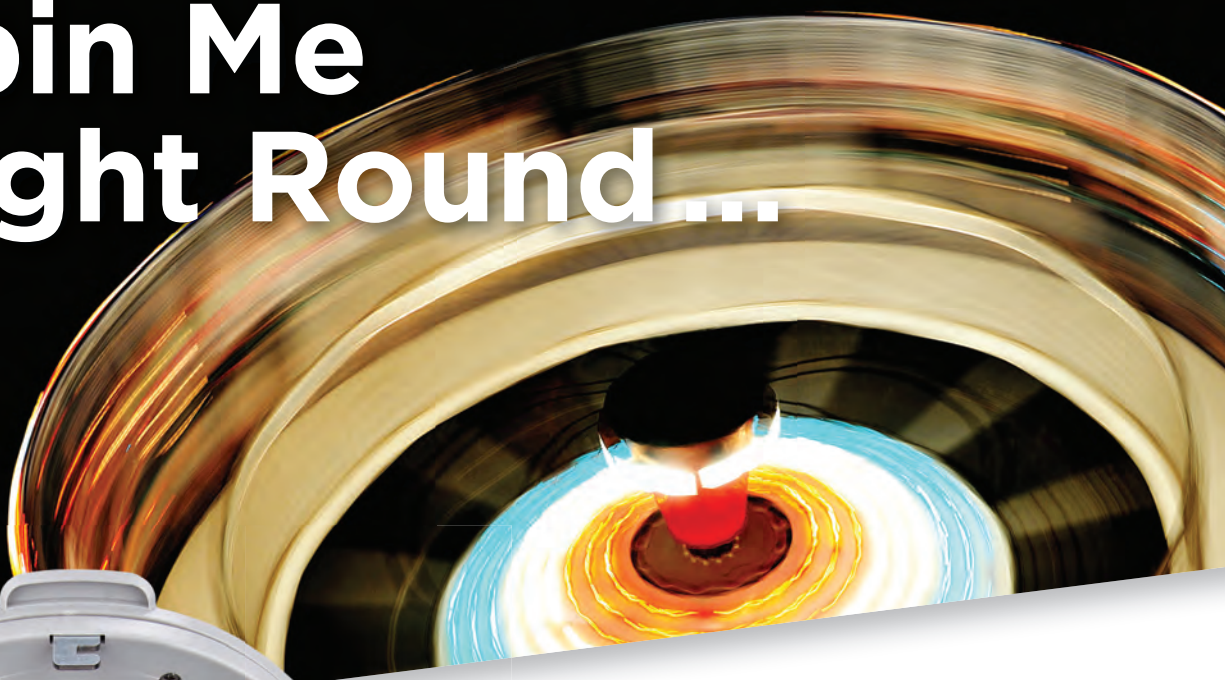

The Only Centrifuge Designed for Glass Autosampler Vials*

High Speed — Quiet Operation

This high speed centrifuge has a specially designed rotor and eight (8) adapters with cushions for approved glass autosampler vials: The MRQ™ (1.2ml) and Max Recovery (1.8ml) single piece (heavy wall) vials. The centrifuge is supplied with one pack of approved MRQ™ screw top vials with RSA-Pro™ surface treated glass for low adsorption of some proteins, screw caps with high purity septa and a wrench for tightening the centrifuge rotor.

The Vial Centrifuge™ offers 16,800xg with a unique air-flow system that keeps your samples cool. This unit features a large, touch panel screen for easy operation which controls and displays actual speed (in rpm or rcf) along with set and remaining spin times. Store up to six (6) speed, time, memory profiles on the "mySpin" display icon for instant recall to get results fast.

The compact design of this centrifuge is cold room safe and only 9"x12"x7.75" taking up less bench space than other centrifuges and carries a two-year manufacturer's warranty.

- » High Speed with Quiet Operation
- » Spin with Organic Solvents
- » Eliminate Extractables

Vials and Caps Kit Included

SPECIFICATIONS	
Dimensions:	9 x 12 x 7.75 in.
Momentary:	Yes
Timer:	1 to 99 min. / cont
Increment:	100 rpm/ 100 rcf
Speed:	1,000 to 13,500 rpm (100 to 16,800 xg)
Electrical:	115V, 60 Hz or 230V, 50 Hz

Visit Today: **mtc-usa.com**

**Use only with authorized vials & caps.*

MICROSOLV TECHNOLOGY CORPORATION

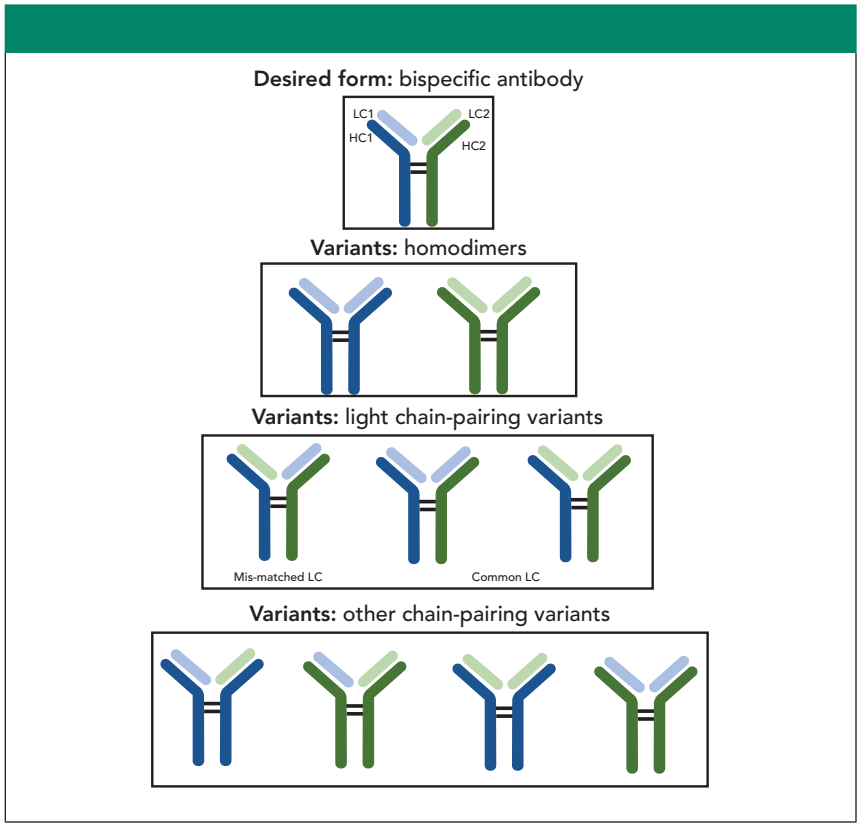

Scheme 1: Potential variants produced during the assembly of a full-length bispecific antibody. LC = light chain. HC = heavy chain.

taneous binding to two cell-surface targets; and 3) bridging IX and X factors in the coagulation cascade for the treatment of hemophilia A (1,3,5).

The concept of bispecific antibodies dates back to the last century (6,7). However, clinical success and large-scale production only became a reality in the past few years (2), coinciding with growing interest in the vast potential of this class of molecules among both the medical and scientific communities (3). That passionate interest spurred tremendous technical advancements in the development, engineering, and production of bispecific molecules. This article focuses on full-length bispecific antibodies and the analytical strategies required to ensure a successful product outcome. An understanding of the potential variants and manufacturing options to reduce their presence is also discussed. In general, there are two strategies to maximize the yield and purity of the desired product: to encourage heterodimerization (increasing the level of desired product), or to facilitate homodimer removal (8).

Strategies to Encourage Correct Chain Pairing

To achieve high yield and purity of the desired product when producing a bispecific antibody, the most effective strategy is to minimize the generation of undesired product variants by encouraging correct chain pairing (8). For a full-length bispecific antibody, there are typically four different polypeptide chains, light chain 1 (LC1), light chain 2 (LC2), heavy chain 1 (HC1), and heavy chain 2 (HC2). When all four polypeptide chains are produced from a single cell, each chain has an equal opportunity to form disulfide bonds with the others. In such a case, one could theoretically generate 10 different products with only one of them being the desired product (1/10) (Scheme 1). One strategy to simplify manufacturing is to reduce the number of possible chains, such as using the common LC or common HC. By reducing the total number of different polypeptide chains to three (common LC, HC1, and HC2; or LC1, LC2 and common HC), the theoretical number of different products reduces to only three. Such a strategy can significantly reduce the possible number of undesired products from nine to two, but may not always be possible due to other considerations, such as desired affinity to target or patent-related considerations.

Another strategy to encourage the formation of the desired product is achieved by introducing specifically designed mutations in the C_H3 domain of the Fc or hinge region of the HCs; these mutations introduce additional features in each HC to encourage heterodimerization and discourage homodimerization. Although the theoretical number of different products in this case is still 10 (9 of which are undesired), the likelihood of forming the desired product is significantly increased. To date, more than a dozen different mutations have been engineered and demonstrated as effective in maximizing the yield of the desired product (9–16). These features include mutations with increased side chain size and hydrophobicity ("knobs") in one HC, matched with another HC with mutations that form hydrophobic "holes" (10). These mutations encourage the desired HC pairing through hydrophobic interactions and discourage the formation of knob–knob homodimers by steric hindrance. This strategy has been used in both single-cell format or two-cell format. For the two-cell format, the two halves of the antibody (LC1 + HC1 and LC2 + HC2) are produced separately in two different cell lines before annealing under a mild in vitro reduction condition (17).

Another example of Fc mutation-driven chain pairing involves the introduction of amino acid mutations containing charged side chains that can form salt bridges between two different HCs (15). Similarly, desired chain pairing between the HC and LC can be facilitated using this strategy (18).

An additional strategy specifically aimed at reducing LC mispairing is the "CrossMab" format, where the HC and LC domains in Fab are swapped (19). This domain swap maintains antigen-binding affinity while reducing the possibility of LC mispairing by making the two

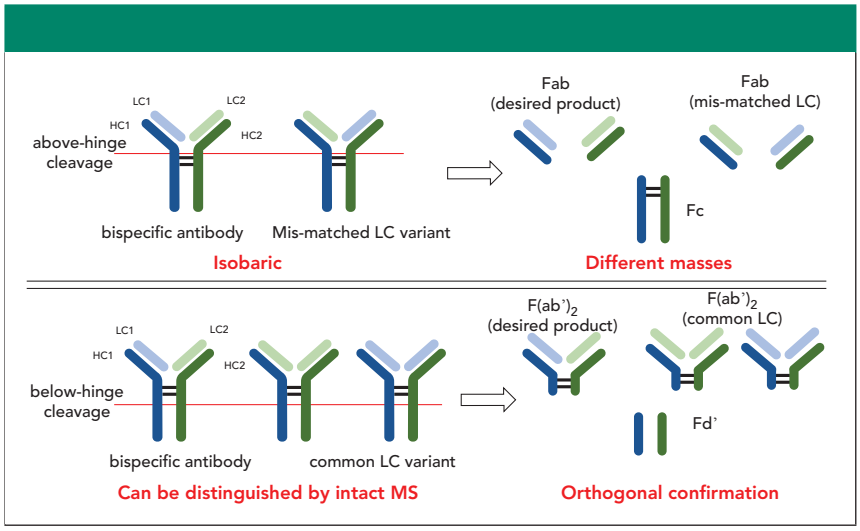

Scheme 2: Strategies for chain-paring variant detection using hinge-specific enzymes.

LCs very different. The main advantage of this strategy is that it can be applied to any two existing full-length antibodies to generate bispecific antibodies without screening for new complementarity-determining region (CDR) sequences.

Currently, these strategies have been employed in several clinical-stage bispecific antibodies.

Strategies to Facilitate the Removal of Homodimers

The undesired products are removed through the purification process as much as possible. If certain forms of the undesired products share many similar characteristics with the desired product, the robust removal of these undesired products during the purification process becomes a challenge. Therefore, it can be ideal to engineer the polypeptide chains in a bispecific molecule to create distinct characteristics, such as hydrophobicity and isoelectric point (pI), so that the undesired products can be more easily separated from the desired product (8).

The purification process of full-length antibodies typically involves three columns (10,11,20). The first is a protein A affinity capture column to extract the antibodies from host cell proteins (HCPs) and other cell culture impurities; noting that full-length antibodies bind to protein A via the Fc region with high specificity. The second and the third columns are called "polishing" columns; their purpose is to further remove HCPs and product-related variants, such as aggregates and fragments. These columns are typically ion-exchange or mixed-mode chromatography columns.

The first affinity capture column can be used to differentiate heterodimer products from the homodimer variants (11). Mutations in the protein A binding region of the Fc domain can be introduced to modulate the binding affinity of bispecific antibody products to the protein A column. As a result, the homodimers have either strong or weak affinity to the protein A column, while the binding affinity of the heterodimer is at an intermediate level.

The latter columns in the purification process have also been exploited to separate desired product from the homodimers (9). One interesting technique introduces mutations in the C_H3 domain of both HCs, so that the pI values of both homodimers are significantly different from that of the heterodimer. The different pI values allow for the complete removal of homodimers through the commonly used ion-exchange column in the purification process. The different pI values are achieved by introducing mutations with charged side-chains (such as lysine or aspartic acid) so that the homodimers bear a different net charge from either homodimer. In large-scale purification processes where bind-and-elute mode is often used, the net charge difference between the desired product and the homodimers should be large enough to allow sufficient removal of the homodimers. When the complete removal of both homodimers by one column step is not possible, other factors, such as the expected safety impact of the homodimers, needs to be considered to achieve optimum purification conditions. For example, if one homodimer is assumed to possess a higher safety risk than the other homodimer, the removal of the former should be prioritized. Meanwhile, the assessment of safety and efficacy impact of both homodimers should be continued as the drug candidate progresses through clinical phases.

Analytical Challenges to Identify and Quantitate Product-Related Variants

Even with advanced manufacturing and purification techniques, identification and quantitation of undesired product variants remains a necessity but can be a difficult challenge for a bispecific antibody, especially in cases where mutations have been introduced (21–23). Mass spectrometry (MS) has been the most capable tool for identifying and quantitating these variants, especially during the early stages of development (23–27). For methods developed to monitor product variants, purified analytes, such as homodimers, are usually required as standards to obtain quantitative results through a standard curve generated by serial dilution or standard addition. Whenever possible, a low quantitation limit and wide dynamic range have been demonstrated using these approaches.

As depicted in Scheme 1, the product-related variants in bispecific antibodies include homodimers and the undesired chain-pairing variants (mismatched LC, common LC, and other chain-pairing variants). The undesired chain-pairing variants can be very challenging to detect and

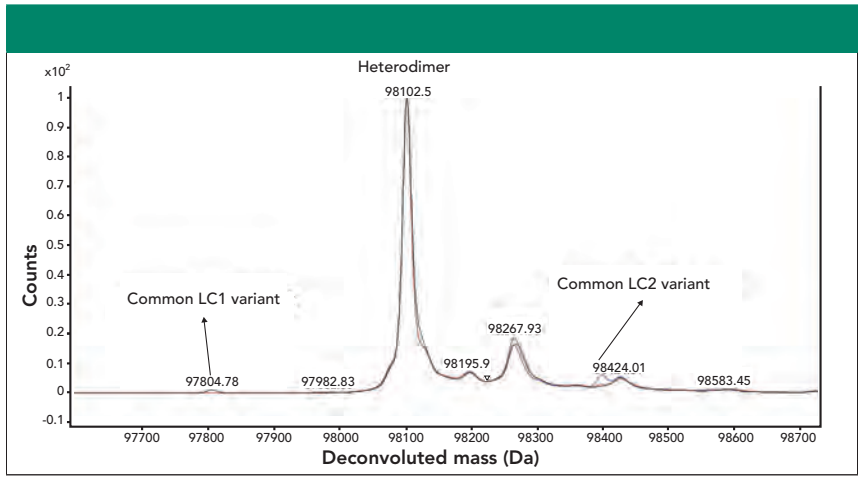

Figure 1: Overlay of deconvoluted mass spectra showing the masses of bispecific antibody A heterodimer with two different common LC variants. Other unlabeled masses are due to expected PTMs of the heterodimer.

quantitate for several reasons. They are usually present at much lower levels relative to the desired product, and may present in a mass region crowded by the expected variants (such as post-translational modifications or PTMs) of the desired product. In such a case, an orthogonal approach such as MS analysis of the subunits is valuable to confirm the presence of the undesired chain-pairing variants. The LC mismatched species (LC1HC2 + LC2HC1) have the added challenge of being structural isomers to the desired product, and cannot be distinguished at the intact or reduced level by MS.

Recent methods that employ hinge-specific proteases (such as IgdE, Kgp, or IdeS) that allow subunit analysis by MS have demonstrated strong potential for the detection and potential quantitation of LC chain-pairing variants (22,24) and a proof-of-concept example will be presented later.

In addition to MS-based methods, chromatography and capillary electrophoresis (CE)-based methods are also widely used for the detection and quantitation of product variants. In the second case study presented here, the homodimers have pI values different from that of the heterodimer, due to the mutations that were introduced to facilitate the removal of homodimers by ion-exchange chromatography. However, the heterodimer is presumed to contain a positive charge patch, thus it is important to consider potential charge-to-charge interactions between the heterodimer and the negatively charged homodimer (homodimer 1). In this case study, we presented the experiments to confirm the linearity of homodimer 1 quantitation that supported a successful qualification of this chromatography-based method for homodimer quantitation.

Case Studies

Detection of Chain-Pairing Variants in Bispecific Antibody A by MS Analysis of Subunits

As discussed in the previous section of this article, the mismatched LC variants and the common LC variants (Scheme 1) can pose a significant challenge in analytical method development. To detect these LC-pairing variants, MS-based analytical assays for bispecific antibody A that involve two different hinge-specific enzymes were developed. As depicted in Scheme 2, the desired product (heterodimer) is isobaric to the mismatched LC variant at both intact and reduced levels.

Upon enzyme treatment, a ~100 kDa subunit of $F(ab)'_2$ containing both LCs and two HC fragments (Fd′) is generated. Given that Fd′ fragments usually bear the majority of the common PTMs, such as N-glycosylation, glycation, and oxidation, the MS spectra in the mass range of the $F(ab)'_2$ subunits can be significantly simplified, allowing the sensitive detection of common LC variants.

Both common LC species (Figure 1) in bispecific antibody A were detected by MS analysis of the subunits, and the results informed the further development of the purification process to successfully remove both common LC species. This assay is suitable for in-process pool and drug substance samples from bispecific antibody A. Mass spectrometry–based relative quantitation can also be performed by comparing the sample to an assay control that contains a known level of the mismatched LC variant.

Method Qualification for an Ion-Exchange Chromatography–Based Assay for Homodimer Quantitation

To facilitate homodimer removal, bispecific antibody B was specifically

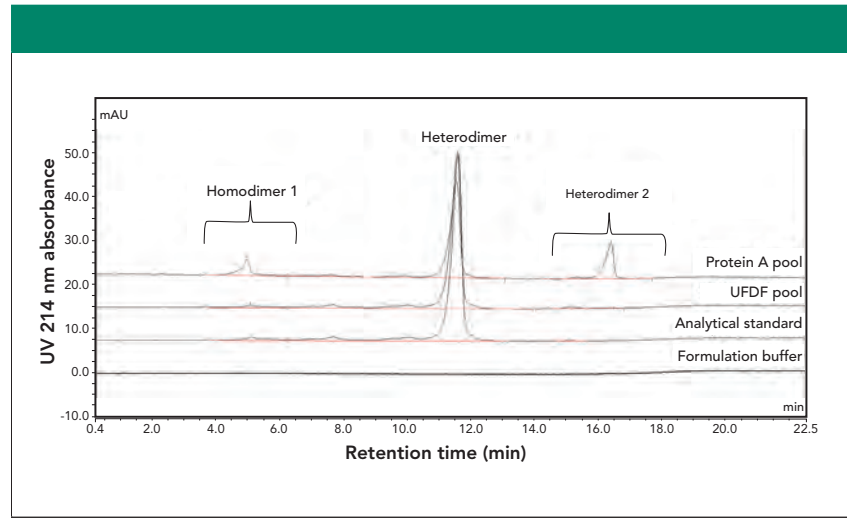

Figure 2: Overlaid chromatograms of bispecific antibody B in (a) protein A process pool, (b) UF/DF pool, (c) analytical standard, and (d) formulation buffer.

engineered so that the two homodimers have different pI values. As a result, an ion exchange chromatography (IEC)–based method employing a pH gradient was developed to monitor homodimers.

This IEC method is suitable for monitoring in-process pool and drug substance samples (Figure 2). Specificity, sensitivity, linearity, precision, accuracy, and autosampler stability were successfully assessed during method qualification. The specificity of the method was demonstrated with no interference was observed by comparing the sample spiked with purified homodimer 1 with formulation buffer. The limit of detection (LOD) of the method is 2% with a wide linear range up to 10% (*w/w*, relative to the heterodimer). The precision of the method was evaluated by two analysts, each making triplicate sample preparations and then running on two instruments using two column batches. The relative standard deviation (RSD) value was 2.0% for the measurement of homodimer 1 concentration relative to the heterodimer. The accuracy of the method was assessed by preparing bispecific antibody B at three concentration levels (50%, 100%, and 150% of target concentration) and spiking homodimer 1 at five concentration levels in formulation buffer (0, 1%, 2%, 5%, and 10%) before injecting each in triplicate. The recoveries for bispecific antibody B and spiked homodimer 1 were observed at 94.9–106.2% and 95.9–99.1%, respectively. In addition, 24 h autosampler stability was demonstrated as no difference in the chromatograms were observed for the initial time-point compared to the 24 h time-point samples.

During the development of the charge heterogeneity method for heterodimer, we observed strong binding of the heterodimer to the cation-exchange chromatography resin. These data indicated the possibility of a positive charge patch on the surface of bispecific antibody B heterodimer. Given that homodimer 1 contains two mutations with negatively charged amino acid residues, a potential range of linearity for homodimer 1 in the presence of the heterodimer was explored. Because homodimer 2 was fully removed by the purification process (determined by a CE-based assay [data not shown]), a similar assessment was not pursued.

In this experiment, we compared the signal-concentration response curves of the purified homodimer 1 spiked from 0 to 10% (*w/w*) into two samples: formulation buffer and a bispecific antibody B analytical standard. The peak area versus homodimer 1 concentration plots are shown in Figure 3. The coefficient of determination (R^2) was greater than 0.999 and the recovery was between 90 and 110% for all levels of homodimer 1 spiked in both formulation buffer and analytical standard. Specificity was further demonstrated by showing that the heterodimer does not interfere with the measurement of homodimer 1 within the studied range. The presumed positive charge patch on the heterodimer does not appear to result in specific charge–charge interactions between the heterodimer and homodimer 1. Therefore, the IEC method is suitable to quantify the homodimer 1 of the engineered bispecific antibody B.

Conclusions

Bispecific antibodies provide new possibilities for drug development along with unique challenges in analytical method development. None of the current manufacturing and purification strategies can ensure 100% heterodimerization, thus analytical methods to detect and measure the levels of undesired product variants are required for the development of bispecific antibodies. Given the unique properties of the product variants, such as chain-pairing variants, product specific analytical methods are often needed. The MS analysis of subunits presented in this article is one of the many possible assay designs. Continued effort from the community is needed to realize further advances in this area. One of the possible directions is to improve the chromatographic resolution of the subunits to allow more accurate quantitation of the variants. Different modes of separation and multidimensional separation can also be explored for this purpose.

On the other hand, the design of bispecific antibodies often involves careful protein engineering. Such engineering requires scientists who are involved in the drug development process to carefully consider the possible impact on the physicochemical properties of the molecule. To ensure the suitability of an assay, assay developers need to anticipate the potential impacts to all aspects of assay performance, and design qualification plans accordingly.

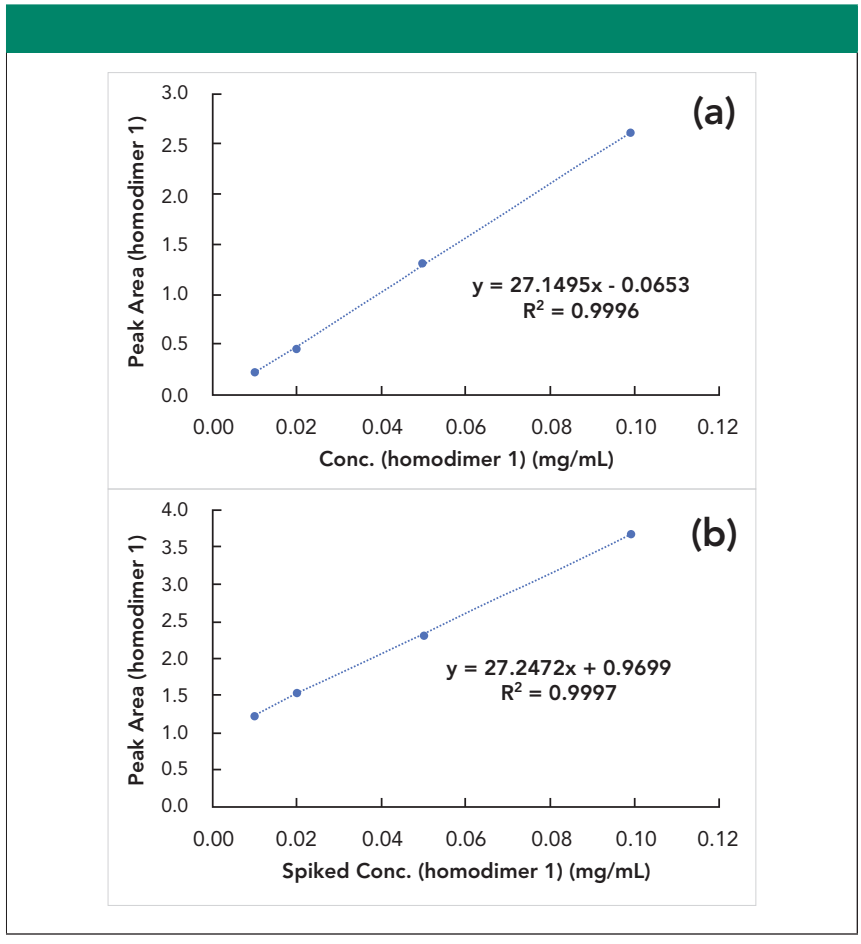

Figure 3: Linearity of the homodimer 1 in the presence of heterodimer. (a) Homodimer 1 peak area versus concentration plot using purified homodimer 1 spiked in formulation buffer; (b) homodimer 1 peak area versus concentration plot using purified homodimer 1 spiked into the heterodimer analytical standard.

Acknowledgments

The authors want to thank Cinzia Stella for providing the opportunity to share our knowledge in this field, and thank Michelle Beardsley for presenting the interesting case of bispecific antibody A to us. We also want to thank Richard Seipert, Jason Gruenhagen, Lu Dai, and Matt Kalo for providing critical review for this article.

References

(1) L Yu and J. Wang, *Cancer Res. Clin. Oncol.* **145**(4), 941–956 (2019).

(2) W.R. Strohl, *Protein & Cell.* **9**(1), 86–120 (2018).

(3) S.E. Sedykh, V.V. Prinz, V.N. Buneva, and G.A. Nevinsky, *Drug Design Devel. Therapy* **12,** 195–208 (2018).

(4) E. Dahlén, N. Veitonmäki, and P. Norlén, *Ther. Advances Vaccines Immunotherapy* **6**(1), 3–17. 2018;

(5) R.E. Kontermann and U. Brinkmann, *Drug Discov. Today.* **20**(7), 838–847 (2015).

(6) G. Riethmüller, *Cancer Immunity* **12,** 12 (2012).

(7) A. Nisonoff and M.M. Rivers, *Arch. Biochem. Biophys.* **93**(2), 460–462. 1961;

(8) U. Brinkmann and R.E. Kontermann, *mAbs* **9**(2), 182–212 (2017).

(9) G.L. Moore, M.J. Bernett, R. Rashid, E.W. Pong, D.-HT. Nguyen, and J. Jacinto, et al., *Methods* **154**, 38–50 (2019).

(10) G. Giese, A. Williams, M. Rodriguez, and J. Persson, *Biotechnol. Progr.* **34**(2), 397–404 (2018).

(11) A.D. Tustian, C. Endicott, B. Adams, J. Mattila, and H. Bak, *mAbs* **8**(4), 828–838 (2016).

(12) S.M. Lewis, X. Wu, A. Pustilnik, A. Sereno, R. Huang, H.L. Rick, et al., *Nat. Biotechnol.* **32,** 191 (2014).

(13) T.S. Von Kreudenstein, E. Escobar-Carbrera, P.I. Lario, I. D'Angelo, K. Brault, J. Kelly, et al., *mAbs* **5**(5), 646–654 (2013).

(14) W. Shatz, S. Chung, B. Li, B. Marshall, M. Tejada, W. Phung, et al., *mAbs* **5**(6), 872–881 (2013).

(15) K. Gunasekaran, M. Pentony, M. Shen, L. Garrett, C. Forte, A. Woodward, et al., *J. Biological Chem.* **285**(25), 19637–19646 (2010).

(16) W. Dall'Acqua, A.L. Simon, M.G. Mulkerrin, and P. Carter, *Biochemistry 37*(26), 9266–9273 (1998).

(17) B. Husain and D. Ellerman, *BioDrugs* **32**(5), 441–464 (2018).

(18) M. Dillon, Y. Yin, J. Zhou, L. McCarty, D. Ellerman, D. Slaga, et al. *mAbs* **9**(2), 213–230 (2017).

(19) W. Schaefer, J.T. Regula, M. Bähner, J. Schanzer, R. Croasdale, H. Dürr, et al. *Proc. Natl. Acad. Sci. USA.* **108**(27), 11187–11192 (2011).

(20) C.L. Young, Z.T. Britton, and A.S. Robinson, *Biotechnol. J.* **7**(5), 620–634 (2012).

(21) L. Schachner, G. Han, M. Dillon, J. Zhou, L. McCarty, D. Ellerman, et al., *C. Anal. Chem.* **88**(24), 12122–12127 (2016).

(22) L.K. Kimerer, T.M. Pabst, A.K. Hunter, and G. Carta, *J. Chromatogr. A* **1601,** 133–44 (2019).

(23) S. Wang, A.P. Liu, Y. Yan, T.J. Daly, N. Li, *J. Pharm. Biomed. Anal.* **154,** 468–475 (2018).

(24) C. Wang, B. Vemulapalli, M. Cao, D. Gadre, J. Wang, A. Hunter, et al., *mAbs* **10**(8), 1226–1235 (2018).

(25) M. Cao, C. Wang, W.K. Chung, D. Motabar, J. Wang, E. Christian, et al., *mAbs* **10**(8), 1236–1247 (2018).

(26) R.J. Woods, M.H. Xie, T.S. Von Kreudenstein, G.Y. Ng, and S.B. Dixit, *mAbs* **5**(5), 711–722 (2013).

(27) F.D. Macchi, F. Yang, C. Li, C. Wang, A.N. Dang, J.C. Marhoul, et al., *Anal. Chem.* **87**(20), 10475–10482 (2015).

Ming Lei is with the Protein Analytical Chemistry group and ***Tao Chen*** is with the Small Molecule Analytical Chemistry group, both at Genentech, Inc., in South San Francisco, California. Direct correspondence to: lei.ming@gene.com.

Size-Exclusion Chromatography for the Analysis of Complex and Novel Biotherapeutic Products

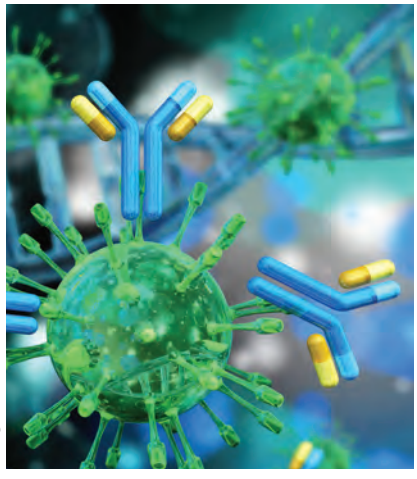

Image credit: ustas/stock.adobe.com

Recombinant biotherapeutics have been produced and marketed for several decades, providing life-changing medicines for a variety of indications. With the maturation of the biotherapeutic market over recent years, novel protein products such as conjugates, bispecifics, fusion proteins, and coformulations are being developed. The detailed characterization and quality control of complex biopharmaceuticals has proven to be more challenging than the typical two-light-chain/two-heavy-chain monoclonal antibody products. This study presents applications of size-exclusion chromatography (SEC) for characterization and quality control of novel biotherapeutic products, including antibody–drug conjugates, hydrophobic proteins, and coformulations. Examples of modifying SEC mobile-phase composition and running conditions to modulate the separation are discussed, as well as approaches and strategies for analyzing atypical protein products such as coformulations.

Jennifer Rea, David Fulchiron, Yun Lou, and Luda Darer

Modern biological drug development stems mostly from using recombinant DNA technology in living microorganisms such as *Escherichia coli* or Chinese hamster ovary (CHO) cells to produce therapeutic agents (1). These recombinant biotherapeutics have been produced and marketed for several decades, providing life-changing medicines for a variety of indications (2). With the maturation of the biotherapeutic market over recent years, novel protein products are now being developed, including antibody–drug conjugates (ADCs) (3), bispecific antibodies (4), and coformulations (5). Although detailed characterization and quality control of biopharmaceuticals are expected for regulatory approval, the physicochemical analysis of novel biotherapeutics with their more complex formats is proving to be more challenging than the more traditional protein products, such as typical two-light-chain/two-heavy-chain recombinant monoclonal antibodies (mAbs).

There are several categories of complex biotherapeutics, and only a few are described in this article. Two-light-chain/two-heavy-chain mAbs are commonly developed as therapeutics because of their specificity to a chosen biological target. ADCs leverage this specificity by having small-molecule drugs attached to a mAb, such that when the mAb binds to a specific target cell, the entire complex is internalized and subsequently releases its small-molecule drug payload into the target cells (3). This approach reduces the chance of off-target side effects, because the potent small-molecule drug is mostly released into target cells. Bispecific mAbs, in turn, simultaneously bind to two targets as a result of different amino acid sequences in each Fab arm—for example, different complementarity determining regions (CDRs) in each antigen-binding fragment (Fab) arm—whereas standard mAbs have the same CDRs in each Fab arm (4). Coformulations are mixtures of two or more differ-

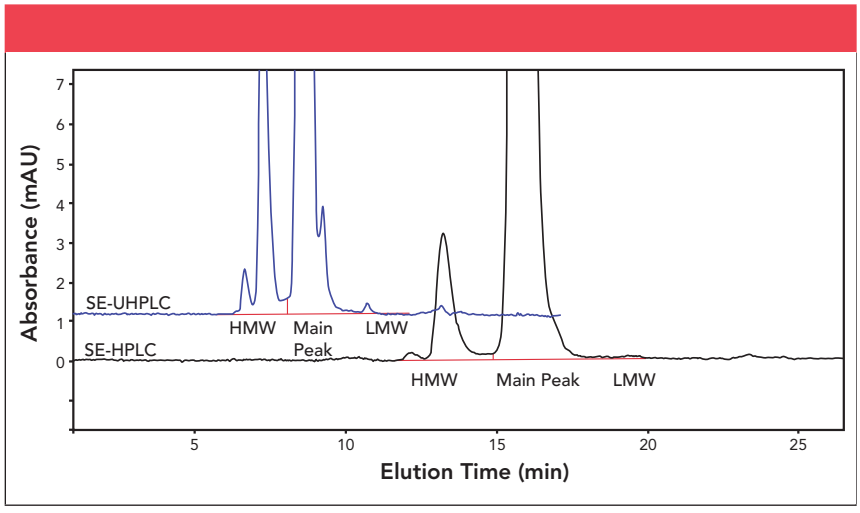

Figure 1: Expanded SE-HPLC and SE-UHPLC profiles of mAb1. Operating conditions for SE-HPLC are similar to those listed in Table I, with the following exceptions: protein load (50 µL of 1 mg/mL mAb1 was injected instead of 200 µg), column temperature (30 °C instead of ambient), and mobile phase (added 10% isopropanol to the mobile phase in Table I). A Tosoh TSKgel G3000SWXL column (7.8 mm x 300 mm, 5-µm) was used for SE-HPLC. Operating conditions for SE-UHPLC are similar to those used in Graf, et al. (11), with the following exceptions: injection volume (10 µL instead of 5 µL), protein concentration (5 mg/mL instead of 10 mg/mL), column temperature (30 °C instead of 25 °C) and mobile phase (added 10% isopropanol to the mobile phase). A Tosoh TSKgel UP-SW3000 column (4.6 mm x 300 mm, 2-µm) was used for SE-UHPLC. High molecular weight forms (HMW), main peak, and low molecular weight forms (LMW) are denoted.

ent active pharmaceutical ingredients (APIs) in the same drug product, thus allowing for simultaneous dosing of multiple drugs and offering both increased convenience to the patient and potential synergistic effects (5). Other complex biotherapeutic formats, such as Fc-fusion proteins, are in clinical development, but are not addressed by this article.

This report covers several applications using size-exclusion chromatography (SEC) to characterize challenging or complex mAb products. SEC is used to separate high molecular weight forms (HMW) or aggregates, from the main peak, which primarily contains the monomeric protein species. To achieve size-based separations, SEC columns are packed with porous material that serves as the stationary phase. In the mobile phase, molecules of various sizes flow into the column, and smaller dissolved molecules flow more slowly through the column, because they penetrate into the pores of the stationary phase, whereas large molecules flow more quickly through the column because they are more excluded from the pores and are eluted in the void volume (6). Consequently, larger molecules are eluted from the column earlier and smaller molecules are eluted later, effectively separating the molecules by hydrodynamic radius, which generally correlates to molecular weight for mAbs.

Size exclusion–high performance liquid chromatography (SE-HPLC) has been the gold standard for size variant analysis for decades (6). SE-HPLC is routinely used in quality control (QC) and development laboratories to quantify protein aggregates, which are of particular concern to health authorities because of their potential to elicit an immunogenic response (7,8). Aggregates and protein fragments may also affect the potency and pharmacokinetics (PK) of the drug product (9). A generic SEC method has been published in the *U.S. Pharmacopeia (USP)* General Chapter <129>, "Analytical Procedures for Recombinant Therapeutic Monoclonal Antibodies," and the recommended conditions are shown in Table I. A major advance in the field of SEC has been the development of

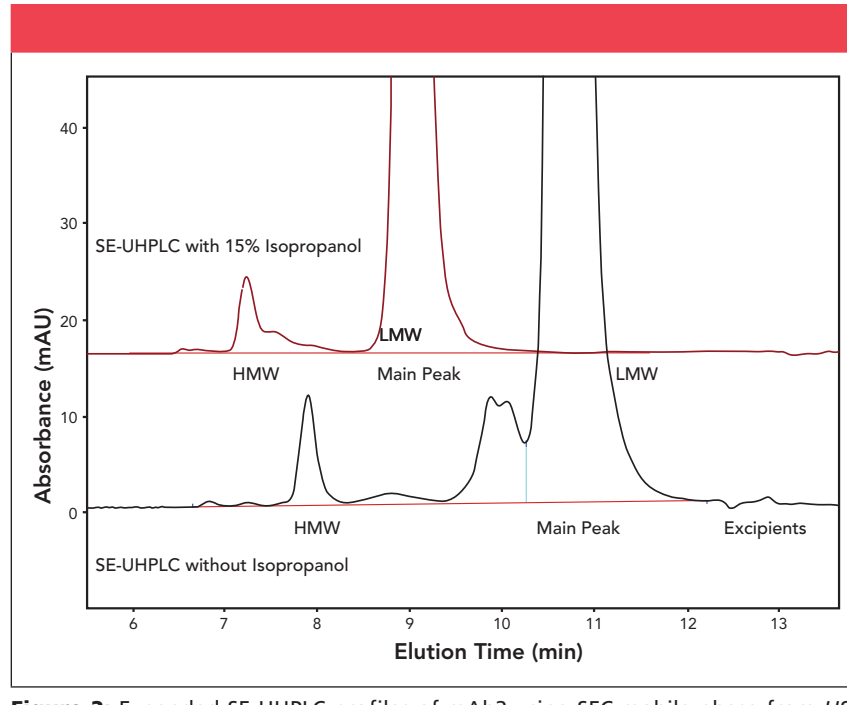

Figure 2: Expanded SE-UHPLC profiles of mAb2 using SEC mobile phase from *USP* <129> with and without 15% isoproponol in the mobile phase. Operating conditions for SE-UHPLC are similar to those used in Graf, et al. (11), with the following exceptions: injection volume (10 µL instead of 5 µL), protein concentration (5 mg/mL instead of 10 mg/mL), column temperature (30 °C instead of 25 °C) and mobile phase (added 15% isopropanol to the mobile phase, where stated). A Tosoh TSKgel UP-SW3000 column (4.6 mm x 300 mm, 2-µm) was used for SE-UHPLC. High molecular weight forms (HMW), main peak, low molecular weight forms (LMW), and excipient region are denoted, where applicable.

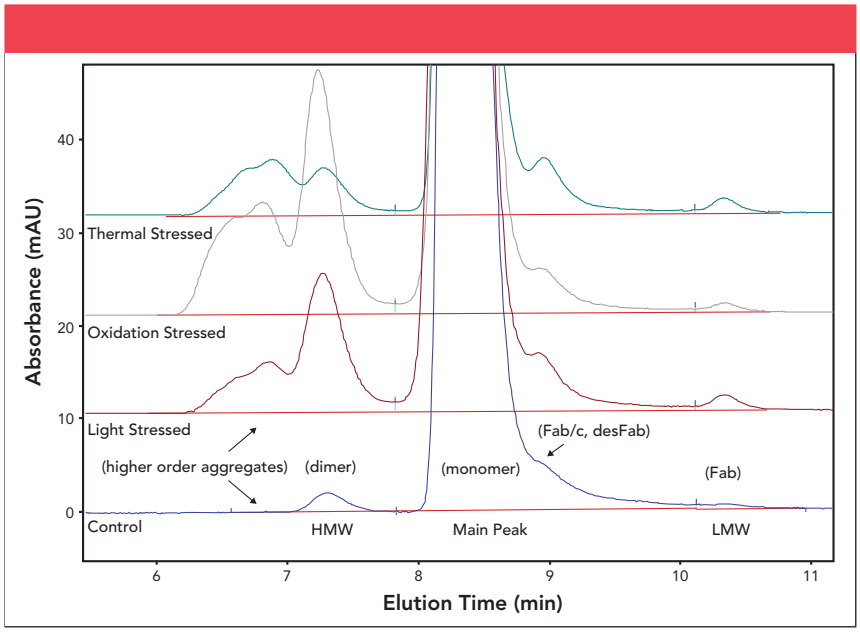

Figure 3: Expanded SE-UHPLC profiles of an ADC (mAb3) using SEC mobile phase from *USP* <129> with 10% isopropanol. Operating conditions for SE-UHPLC are similar to those used in Graf, et al. (11), with the following exceptions: injection volume (10 µL instead of 5 µL), protein concentration (5 mg/mL instead of 10 mg/mL), and mobile phase (added 10% isopropanol to the mobile phase). A Tosoh TSKgel UP-SW3000 column (4.6 mm x 300 mm, 2-µm) was used for SE-UHPLC. High molecular weight forms (HMW), main peak, and low molecular weight forms (LMW) are denoted. Peak identities (monomer, dimer, higher order aggregates, Fab/c (desFab), and Fab) are denoted in parentheses. Due to lack of adequate resolution, that is, no clear valley between peaks, the Fab/c peak is grouped with main peak for the control.

size exclusion–ultrahigh-pressure liquid chromatography (SE-UHPLC), which utilizes instrumentation featuring decreased system volume and higher allowable backpressures compared to typical HPLC instruments. SE-UHPLC has been demonstrated for high-throughput, high-resolution applications (10), and has been validated for use in QC laboratories (11). Figure 1 demonstrates the improvements in speed and resolution of a monoclonal antibody (mAb1) separated by SE-UHPLC relative to SE-HPLC. HMW forms are eluted before the main peak and low molecular weight forms (LMW) are eluted after the main peak. Note that peak integration strategy may vary from product to product (for example, continuous flat baseline versus continuous valley-to-valley baseline versus discontinuous peak-to-peak baseline), but different integration strategies may be acceptable as long as they are adequately justified (for example, a slanted baseline may cause a discontinuous baseline to be more accurate than a continuous flat baseline). In Figure 1, note that the SE-UHPLC fragment peak after the main peak is grouped with the main peak. This grouping is done to obtain similar relative peak area quantification with the SE-HPLC method, which does not resolve this fragment peak from the main peak.

Although the SE-HPLC method in *USP* Chapter <129> is suitable for many mAbs, the examples in this article will demonstrate that the *USP <129>* method may not be optimal for every biotherapeutic product. In these cases, a variety of strategies may be employed to improve the SEC separation, such as changing the mobile-phase composition or switching from the HPLC version (the *USP* <129> method) to the UHPLC version to increase the resolution between size variant peaks. Detailed method development and troubleshooting of SEC methods are not covered in this article; rather, this article focuses on various complex and novel protein products (ADCs, hydrophobic proteins, bispecific antibodies, and coformulations) that benefit from advanced understanding of SEC separations and improved column and instrument technologies to enable better resolution and improved quantitation of protein size variants.

Materials and Methods

Columns and Chemicals

SE-HPLC experiments were performed using a Tosoh TSKgel G3000SWXL

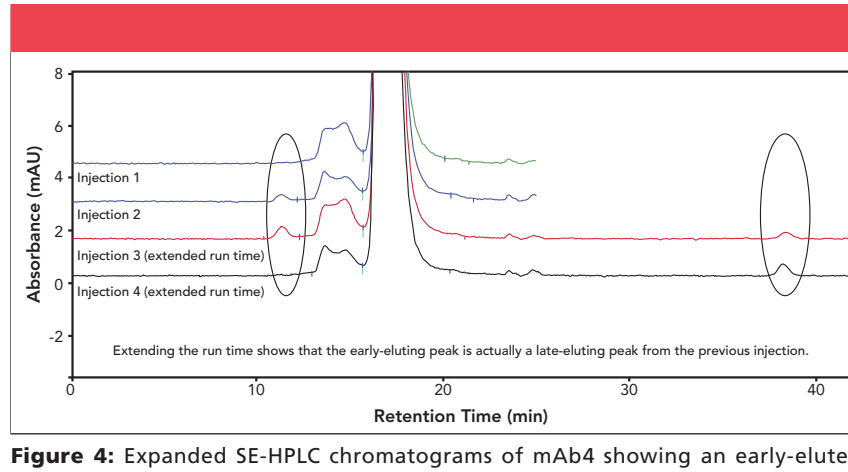

Figure 4: Expanded SE-HPLC chromatograms of mAb4 showing an early-eluted peak visible in second injection using a 25-min isocratic SEC method with organic solvent in the mobile phase. A late-eluted peak become evident in third injection after extending the run time. The fourth injection no longer shows an early-eluted peak. Peak was identified as a leachable from plastic storage containers. Operating conditions are similar to those listed in Table I, with the exception of protein load (50 µg of mAb was injected instead of 200 µg) and mobile phase (added 15% isopropanol to the mobile phase). A Tosoh TSKgel G3000SWXL column (7.8 mm x 300 mm, 5-µm) was used for SE-HPLC.

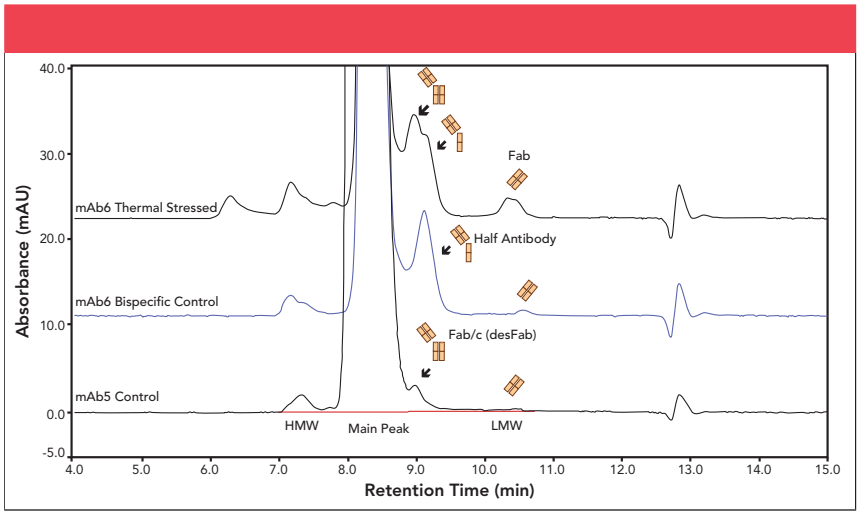

Figure 5: Expanded SE-UHPLC profiles of mAb5 (standard mAb) and mAb6 (bispecific mAb). Operating conditions for SE-UHPLC are similar to those used in Graf, et al. (11), with the following exceptions: injection volume (10 µL instead of 5 µL) and protein concentration (5 mg/mL instead of 10 mg/mL). A Tosoh TSKgel UP-SW3000 column (4.6 mm x 300 mm, 2-µm) was used for SE-UHPLC. High molecular weight forms (HMW), main peak, and low molecular weight forms (LMW) are denoted. Antibody fragments eluting immediately after the main peak are illustrated.

column, 7.8 mm x 300 mm, 5-µm. SE-UHPLC experiments were performed using either a Waters Acquity BEH200 SEC column, 4.6 mm x 300 mm, 1.7-µm, or a Tosoh TSKgel UP-SW3000 column, 4.6 mm x 300 mm, 2-µm.

Monoclonal antibodies were produced in-house at Genentech. The thermally stressed sample for mAb3 was produced by incubating mAb3 at 40 °C for 14 d. The oxidation stressed sample for mAb3 was produced by incubating mAb3 with 1.6 mM AAPH (2,2'-azobis(2-amidinopropane) dihydrochloride) for 24 h at 40 °C. The light-stressed sample for mAb3 was produced by subjecting mAb3 to 1.36 million lux hours (M lux h) for a duration of 24 h. The thermally stressed sample for mAb5 was produced by incubating mAb5 at 40 °C for four weeks. Common buffers, salts and solvents were procured from Fisher Scientific or VWR.

Equipment

SE-HPLC chromatographic experiments were performed on either an Agilent 1100/1200/1260 HPLC instrument or a Waters 2695(e) HPLC system. SE-UHPLC chromatographic experiments were performed on either a Waters Acquity H-Class UPLC or a ThermoScientific UltiMate 3000 RSLC system. Components of the system included a high-pressure gradient binary pump (ThermoScientific RSLC) or a low-pressure gradient quaternary pump (Waters UPLC), a column compartment capable of temperature control, an autosampler with sample temperature control capability, and a tunable UV-vis detector. Instrument control, data acquisition, and compilation of results were performed using ThermoScientific Chromeleon software.

Methods

SE-HPLC was performed using the SEC method conditions published in the *USP* Chapter <129>, "Analytical Procedures for Recombinant Therapeutic Monoclonal Antibodies," (Table I), unless otherwise indicated. SE-UHPLC was performed using the SE-UHPLC method conditions published by Graf and associates (11), unless otherwise indicated.

MAb samples were diluted with mobile phase and kept at a temperature of 5 °C ± 3 °C in the autosampler. The column effluent was monitored at 280 nm. A blank injection was performed with each sequence prior to sample injection. After the installation of a new column, conditioning runs were performed until consistent profiles were achieved. Each chromatogram was carefully integrated to ensure that only peaks not present in the associated blank were considered to be protein (ThermoScientific Chromeleon software).

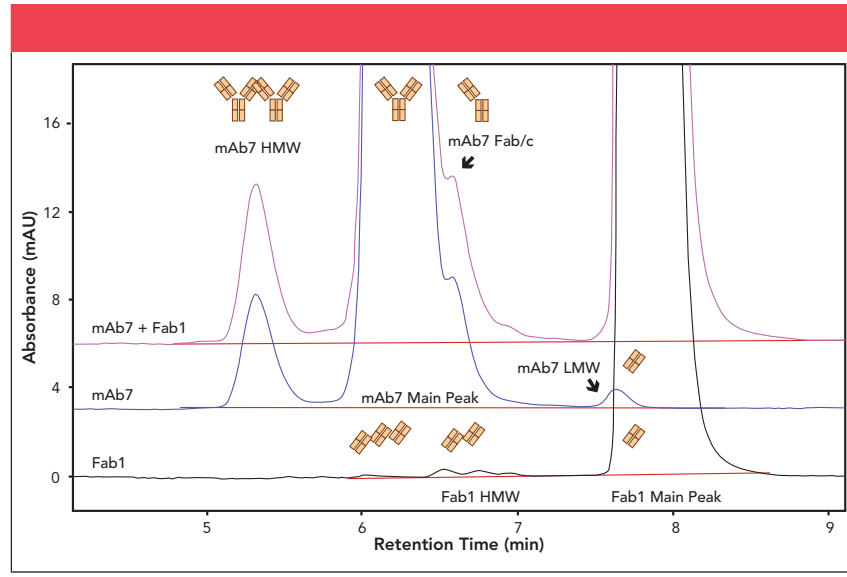

Figure 6: Expanded dual-column SE-UHPLC profiles of a mAb/Fab co-formulation (mAb7 + Fab1). Operating conditions for SE-UHPLC are as follows: flow rate = 0.2 mL/min, run time = 40 min, column temperature = 40 °C, protein concentration = 14 mg/mL mAb 7 and 5 mg/mL Fab1. Two Waters Acquity BEH200 SEC columns (4.6 mm x 300 mm, 1.7-µm) connected in series were used for SE-UHPLC. High molecular weight forms (HMW), main peak, and low molecular weight forms (LMW) are denoted for each molecule. Monoclonal antibody size variants are illustrated.

Table I: Recommended SEC operating conditions from *USP* <129>

Parameter	Operating Conditions
Column dimensions	300 mm x 7.8 mm; 5-µm
Column temperature	Ambient
Injection volume	20 µL
Run time	30 min
Autosampler temperature	Maintain at 2–8 °C.
Detection wavelength	UV 280 nm
Flow rate	0.5 mL/min
Mobile phase composition	Prepare by mixing 10.5 g of dibasic potassium phosphate, 19.1 g of monobasic potassium phosphate, and 18.6 g of potassium chloride per L of water. Verify that the pH is 6.2 ± 0.1. Pass through a membrane filter of ≤ 0.45-µm or smaller pore size.
Sample solution	Dilute the sample to 10 mg/mL in mobile phase if dilution is required. Similarly, a blank should be prepared using an equivalent dilution of formulation buffer in the mobile phase.
System suitability solution	Prepare a 10 mg/mL USP Monoclonal IgG System Suitability RS solution in mobile phase by reconstituting the contents of one vial with 200 mL of mobile phase. Reconstituted system suitability solution should be used within 24 h after reconstitution, and should be stored at 2–8 °C if not used immediately.
System suitability blank	Use mobile phase.

ADCs and Hydrophobic Proteins

Although SEC serves as a primarily size-based separation method, SEC has also been demonstrated to separate species based on hydrophobicity due to the interaction of the analytes with the stationary phase (12). These secondary interactions sometimes result in undesired increases in elution time and peak tailing, which may be mitigated by mobile phase additives. For example, the addition of organic modifiers has been shown to reduce hydrophobic interactions between the protein analytes and the stationary phase (13). Figure 2 shows a hydrophobic mAb analyzed by SE-HPLC with and without the use of an organic modifier (15% isopropanol). The addition of the organic modifier decreases the main peak elution time and alters the peak profile. It should also be noted that the main peak width decreased with the addition of organic solvent to the mobile phase. Therefore, organic modifier in the mobile phase may be explored if peak broadening or peak tailing is significant for the main peak.

ADCs generally have increased hydrophobicity compared to a standard mAb as a result of the hydrophobic linker drugs attached to the mAb. Thus, an SE-UHPLC method with 10% isopropanol in the mobile phase was developed to mitigate the hydrophobic interactions between the ADC and the stationary phase (Figure 3). Upon different degradative stresses, the relative peak area of the HMW forms increase compared to the control. Peaks representing higher order aggregates (in other words, larger than dimer) increase significantly upon different degradative stress conditions and elute earlier than the main HMW forms (dimer).

While the use of an organic modifier in the SEC mobile phase can be helpful for improving resolution for hydrophobic analytes, addition of organic solvent may cause leachables from plastic containers to be eluted off the column and subsequently appear in the SEC chromatograms as new peaks. Given that leachables are small, they are eluted well after the analytes of interest, and a method that is too short would cause the leachables to appear in subsequent runs (Figure 4). In this instance, further characterization determined that the peak was a leachable generated from prolonged storage of sample in polypropylene tubes, and that organic solvent in the mobile phase caused the leachable to be eluted off the column. Indeed, organic solvents such as isopropanol are also used as extraction solvents during extractable studies (14). Therefore, careful consideration of sample container materials may be needed to avoid new, undesired peaks resulting from leachables.

Bispecific Antibodies

As described previously, bispecific antibodies are designed to simultaneously bind to two different epitope targets due to the different amino acid sequences in each Fab arm. In some cases, one Fab arm of the bispecific antibody may be longer than the other Fab arm (11). Unlike standard mAbs, bispecific antibody products have unique but undesirable product variants such as homodimer (both Fab arms bind to the same target), mispaired or scrambled light chain, and single arm half-antibodies (15). Some of these variants may be resolved using SEC, with SE-UHPLC resulting in better resolution of these bispecific variants compared to SE-HPLC (11).

In one study, SEC directly coupled to native mass spectrometry (SEC–MS) was developed to rapidly characterize a bispecific antibody and its variants (15). Generally, SEC methods do not have sufficient resolving power to resolve size variants of similar masses; however coupling MS to native SEC (SEC–MS) can be used to identify noncovalent and covalent size variants with similar elution times. This tool is of particular importance for bispecific antibodies, because bispecific aggregates and fragments often have similar SEC elution times as their homologous homodimer variants, thus requiring an orthogonal technique (in this case, MS) to identify the peaks of interest.

Because bispecific molecules have different types of size variants than traditional mAbs as a result of their

asymmetrical structure (two different antibody halves in one mAb), their SEC profiles tend to have different peak profiles than traditional mAbs. The arrows in Figure 5 show fragment peaks eluted at different times for the standard mAb and the bispecific mAb. These differences result from the fact that the fragment in the mAb profile is Fab/c (otherwise known as a *desFab* or *one-armed antibody*), whereas the fragment in the bispecific mAb profile is primarily half antibody, which has a lower molecular weight and later elution time than the Fab/c fragment. Thermally stressing the bispecific mAb produces more Fab/c fragment, and the Fab/c and half-antibody peaks in the stressed sample profile can be partially resolved by SE-UHPLC (Figure 5).

Coformulation of Multiple Protein Products

With an increasingly diverse selection of mAb products in development and on the market, combination therapies of multiple biotherapeutics are being developed, further leveraging the wide selection of biotherapeutics available to treat complex diseases. Combination mAb therapies can be sequentially administered at the clinic (one drug after another) or co-administered (two drugs in the same IV bag). For increased patient convenience, some manufacturers are moving toward coformulated drug products where two or more biotherapeutics are combined in the same vial and released by the manufacturer for shipment to the clinic (5). While the coformulated drug product is more convenient for the patient, it can be challenging for the manufacturer to develop analytical methods and specifications to ensure acceptable product quality of each individual drug in the comixed product (16).

A typical SEC method, such as the *USP* <129> SE-HPLC method, can be used to analyze coformulated or comixed biotherapeutics (16). However, the resolution of the *USP* <129> method may not be adequate for product quality assessment in a coformulation, particularly for two drugs having similar molecular weights. In these cases, various strategies may be employed to further increase the resolution to enable quantitation of the size variants in the coformulated drug product. For instance, an analyst may switch to SE-UHPLC or multiple SE-UHPLC columns in series to further improve the separation (17). Figure 6 shows the chromatograms obtained from a mAb + Fab (antibody fragment) coformulation using dual-column or tandem SE-UHPLC (for example, two columns connected in series). Although not all peaks are fully resolved, tandem SE-UHPLC provides better resolution than single-column SE-HPLC. For degraded mAb + Fab samples (not shown), it may be difficult to determine by SEC which product variant from either mAb7 or Fab1 has increased in the overlapping peak regions. SEC-MS (15) or SEC with multi-angle light scattering (SEC-MALS) (16) can be

employed to elucidate the identities of the product variants in degraded coformulation samples, and SEC-MS may provide relative quantities of the product variants in the overlapping peak regions. With this information, the likely degradation pathway of the coformulated product may be predicted, and the tandem SE-UHPLC method may be used to monitor the size variants of the coformulated product based on the predicted degradation pathway. In other words, although the tandem SE-UHPLC method may not resolve all size variants, the improved resolution and knowledge of the degradation pathway may be leveraged to interpret results from accelerated stress studies or real-time stability studies.

Discussion and Conclusion

This article presents examples of SEC analysis of novel biotherapeutic products, which are generally more complex than traditional mAbs. Specifically, we covered hydrophobic molecules, ADCs, bispecific mAbs, and coformulations, all which have unique considerations when developing and performing SEC methods. For hydrophobic molecules and ADCs, we demonstrated that adding organic modifier in the mobile phase reduced elution time of the main peak because of the disruption of the hydrophobic interaction between the protein and the stationary phase. We also showed that the addition of organic modifier can alter the peak pattern of the SEC separation. Therefore, one must use caution when adding organic solvent to the mobile phase, as unwanted changes to the peak pattern may occur in addition to the desired improvements in elution time and resolution.

Bispecific molecules and coformulations generally have more size variants than standard mAbs. Bispecific molecules may have unwanted half-antibody in the sample that SEC can resolve from Fab/c (desFab) and Fab. Coformulated drug product samples have roughly twice as many product variants as a single API drug product. Because bispecific antibodies and coformulations have more variants to resolve, improved resolution in SEC analyses may be required for thorough physicochemical characterization of the product. In addition to the strategies presented here, other techniques, such as multidimensional LC (18), may be developed to achieve improved peak separation.

The rapid development of biotherapeutics has resulted in increasingly complex products, including ADCs, bispecific mAbs, and coformulations. Size-exclusion chromatography techniques have also improved to allow for better resolution, faster run times, and improved characterization of these analytically-challenging formats. Here we presented examples of SEC approaches for the analysis of ADCs, hydrophobic mAbs, bispecific mAbs, and coformulations. These examples demonstrate that although a generic SEC method has been published in the pharmacopeia, additional SEC method development may be required for the analysis of complex biotherapeutics.

Acknowledgments

The authors would like to acknowledge Armando Cordoba for his technical input, Adithi Bhargava and Lucy Li in Pharmaceutical Development for generating stressed samples, David Michels and Matt Kalo for reviewing this manuscript, and the global Roche/Genentech SEC Analytical Expert Team (AET) for fruitful discussions and collaboration.

References

(1) 1. J.M. Reichert, C.J. Rosensweig, L.B. Faden, and M.C. Dewitz, *Nature Biotech.* **23**(9), 1073–1078 (2005).
(2) A. Philippidis, *Genetic Engineering and Biotechnology News* (March 11, 2019).
(3) N. Diamantis and U. Banerji, *Br. J. Cancer* **114**(4), 362–367 (2016).
(4) S.E. Sedykh, V.V. Prinz, V.N. Buneva, and G.A. Nevinsky, *Drug Des. Devel. Ther.* **12,** 195–208 (2018).
(5) M. Cao, N. De Mel, A. Shannon, M. Prophet, C. Wang, W. Xu., B. Niu, J. Kim, M. Albarghouthi, D. Liu, E. Meinke, S. Lin, X. Wang, and J. Wang, *mAbs* **11**(3), 489–499 (2019).
(6) P. Hong, S. Koza, and E.S.P. Bouvier, *J. Liq. Chromatogr. Rel. Technol.* **35,** 2923–2950 (2012).
(7) T. Uchino, Y. Miyazaki, T. Yamazaki, and Y. Kagawa, *J. Pharm. Pharmacol.* **69**(10), 1341–1351 (2017).
(8) W. Jiskoot, G. Kijanka, T.W. Randolph, J.F. Carpenter, A.V. Koulov, H.-C. Mahler, M.K. Joubert, V. Jawa, and L.O. Narhi, *J. Pharm. Sci.* **105,** 1567–1575 (2016).
(9) J. Vlasak and R. Ionescu, *mAbs* **3,** 253–263 (2011).
(10) E.S.P. Bouvier and S.M. Koza, *Trends in Anal. Chem.* **63,** 85-94 (2014).
(11) T. Graf, R. Ruppert, A. Knaupp, G. Hafenmair, S., Violini, and S. Kiessig, *LCGC North Amer.* **36**(12), 870–879 (2018).
(12) J.A. Pavon, X. Li, S. Chico, U. Kishnani, S. Soundararajan, J. Cheung, H. Li, D. Richardson, M. Shameem, and X. Yang, *J. Chromatogr. A* **1431,** 154–165 (2016).
(13) T. Arakawa, D. Ejima, T. Li, and J.S. Philo, *J. Pharm. Sci.* **99,** 1674–1692 (2010).
(14) D.L. Norwood, D. Paskiet, M. Ruberto, T. Feinberg, A. Schroeder, G. Poochikian, Q. Wang, T.J. Deng, F. DeGrazio, M.K. Munos, and L.M. Nagao, *Pharm. Res.* **25**(4), 727–739 (2008)
(15) M. Haberger, M. Leiss, A.K. Heidenreich, O. Pester, G. Hafenmair, M. Hook, L. Bonnington, H. Wegele, M. Haindl, D. Reusch, and P. Bulau, *mAbs* **8,** 331–339 (2016).
(16) Z.W.K. Glover, L. Gennaro, S. Yadav, B. Demeule, P.Y. Wong, and A. Sreedhara, *J. Pharm. Sci.* **102**(3), 794–812 (2013).
(17) S. Fekete, A. Beck, J.-L. Veuthey and D. Guillarme, *J. Pharm. Biomed. Anal.* **101,** 161–173 (2014).
(18) A. Ehkirch, A. Goyon, O. Hernandez-Alba, F. Rouviere, V. D'Atri, C. Dreyfus, J.-F. Haeuw, H. Diemer, A. Beck, S. Heinisch, D. Guillarme, and S. Cianferani, *Anal. Chem.* **90,** 13929–13937 (2018).

Jennifer Rea, David Fulchiron, Yun Lou, Luda Darer are with Genentech, in South San Francisco, California. Direct correspondence to: rea.jennifer@gene.com

Ferritin as a Natural Protein Scaffold: Building a Multivalent Ferritin–Fab Conjugate

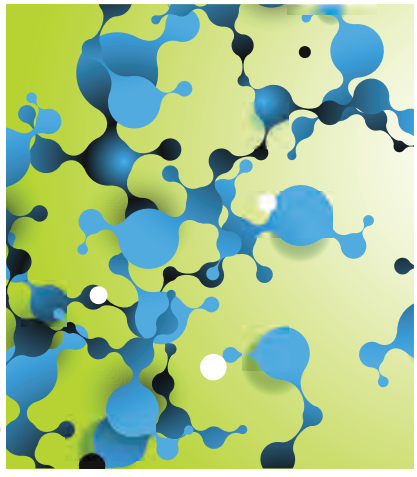

Image credit: Leonid/stock.adobe.com

The design of molecules with a high degree of valency can be useful for receptor clustering, T-cell recruiting, agonist activation, and half-life extension. Although this is traditionally accomplished using polymer-based molecular scaffolds, biocompatibility and the fate of polymer by-products are often of concern. Multivalent, self-assembling scaffolds such as ferritin, a ubiquitous protein found in most human cell types in addition to invertebrates, higher plants, fungi and bacteria, offer an attractive "natural" alternative to polymer-based scaffolds. In mammals, ferritins are composed of 24 subunits that form an icosahedron with an external hydrodynamic radius of 6 nm, and an overall molar mass of approximately 474 kDa, depending on the biological tissue from which it is derived. The utility of molecular cages, such as ferritin and its derivatives for applications in drug delivery, is well-known. Here, we describe the design, production, and characterization of a multimeric ferritin–antibody fragment conjugate. Following optimization of the conjugation strategy using LC–MS, in-depth characterization was performed using SEC-MALS-QELS. The combined results of this study confirmed that Ferritin–Fab conjugates were successfully generated.

Whitney Shatz, Craig Blanchette, Patrick Holder, Robert F. Kelley, Remo Perozzo, and Yogeshvar N. Kalia

There is a growing trend within the field of biotherapeutics to develop molecules with a high degree of valency (1,2). Ferritin family proteins, found ubiquitously in nature, possess many attractive features for the delivery of biotherapeutics (3–6). Ferritin is made up of 24 subunits held together by non-covalent interactions, arranged in an icosahedral cage with 2, 3, and 4-fold axes of symmetry around a central cavity (7,8). While, in nature, the ferritin cavity is used to store and enucleate iron, it can also be repurposed for the encapsulation of drugs or dyes (9). Below pH 3, the ferritin assembly may then be dissociated and reconstituted (10), enabling drugs to be trapped inside the protein "cage" (11). Encapsulation of molecules such as cisplatin (12,13), carboplatin (14), oxaliplatin (15), ruthenium (16,17), and gold (18,19) has been achieved using various ferritin cage disassembly or reassembly procedures. More recently, it was used for the delivery of cisplatin, but without the use of an encapsulation protocol (20). In this case, the interaction was attained through ligand-metal chemistry (21,22), with the preparation of a 1:1 complex between cisplatin and the monomeric subunits of the human ferritin cage (11). Thus, ferritin proteins are attractive vectors for the delivery of drug molecules, either through encapsulation in the central cavity, or through display of drug molecules on the external surface (23). The latter can be achieved using molecular engineering techniques, including the addition of a peptide or protein tag (24).

However, to the authors' knowledge, there are no examples of adapting ferritin for delivery of multimerized antibody fragment (Fab) therapeutics via chemical conjugation. Here, we describe a drug delivery system using ferritin to multimerize a Fab therapeutic. Commercially available horse spleen ferritin (HSF), with its iron core removed (Millipore

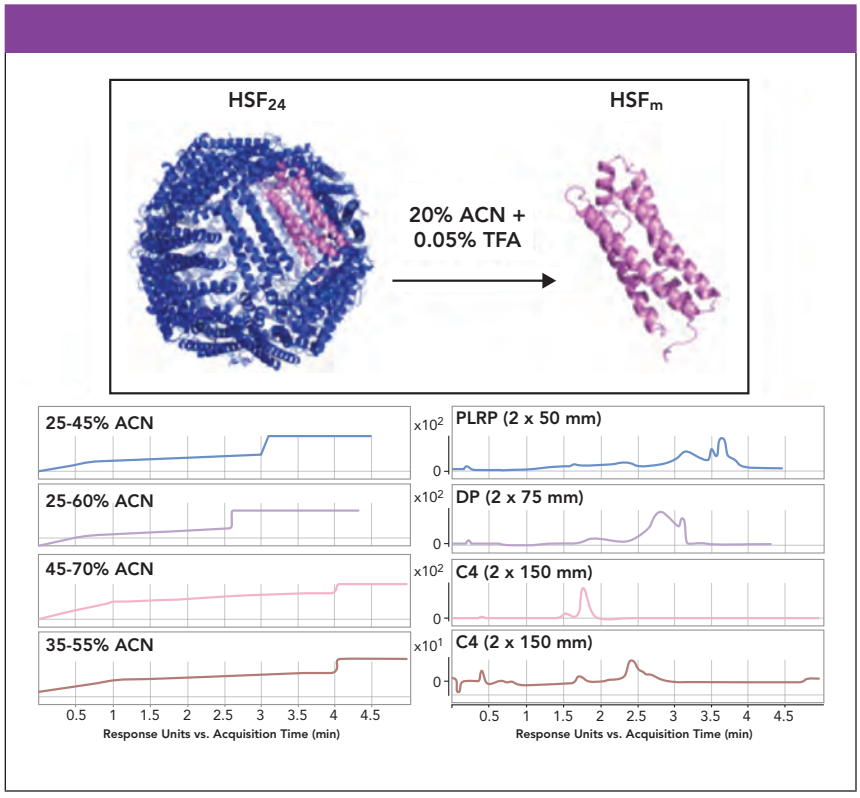

Figure 1: Top panel shows the structure of the assembled icosahedral cage (HSF_{24}) and the denaturing conditions used for its dissociation into the monomer (HSF_m). The lower panel compares gradients and corresponding chromatographic traces of the absorbance at 280 nm for the reversed-phase conditions tested. Note: ACN is acetonitrile, TFA is trifluoroacetic acid, PLRP is is a rigid macroporous styrene and divinylbenzene (PS/DVB) HPLC phase, DP represents a diphenyl (DP) bonded phase, and C4 refers to hydrophobic alkyl chain length of the stationary phase.

Sigma SKU# A3641), was chemically linked through solvent exposed native amino acids to a human Fab. The conjugation strategy was optimized based on analysis, using liquid chromatography in-line with a mass spectrometry detector (LC–MS), while characterization of the resulting conjugates was performed using size exclusion chromatography (SEC) in-line with a multi-angle light scattering detector (MALS) and quasi-elastic light scattering detector (QELS). The results of this study confirmed Fab was successfully conjugated to the HSF cage via site-specific conjugation of the C-terminal cysteine (Cys) on the Fab to solvent exposed lysines on HSF.

Results and Discussion

The first step in developing the conjugation protocol was optimization of the reversed-phase method to enable monitoring of the conjugation reactions. Three different reversed-phase columns and four different gradient conditions were scouted (Figure 1). Based on this analysis, a C4 column (Waters, Acquity UHPLC Protein BEH C4) with a 35%–55% acetonitrile (ACN) gradient resulted in optimal baseline resolution of ferritin (around 2.5 min) from the other impurities in the sample, predominantly the contaminant at around 1.75 min (Figure 1, bottom right panel). While chromatographic separation was achieved, the unambiguous identification of the earlier eluting contaminant was not accomplished. However, the deconvoluted mass from the LC–MS spectrum suggested that it was related to HSF (data not shown).

HSF and Fab were conjugated using a two-step procedure: the first involved attachment of a heterobifunctional linker to each component, and this was followed by secondary conjugation using copper-free click chemistry. In each reaction, the reversed-phase method described above was used to characterize intermediate products (Figure 2). All reactions were incubated at room temperature for 18–24 h. To activate HSF, we chose a heterobifunctional *N*-hydroxysuccinimide (NHS), trans-cyclooctene (TCO), PEG4 linker (NHS-TCO, Figure 2) (BroadPharm, BP-22418). Three different molar excesses of linker (3:1, 20:1, 100:1) relative to HSF monomer (HSF_m) were evaluated and monitored by LC–MS (Figure 3a–3d) to generate the HSF displaying a TCO functional group (HSF-TCO).

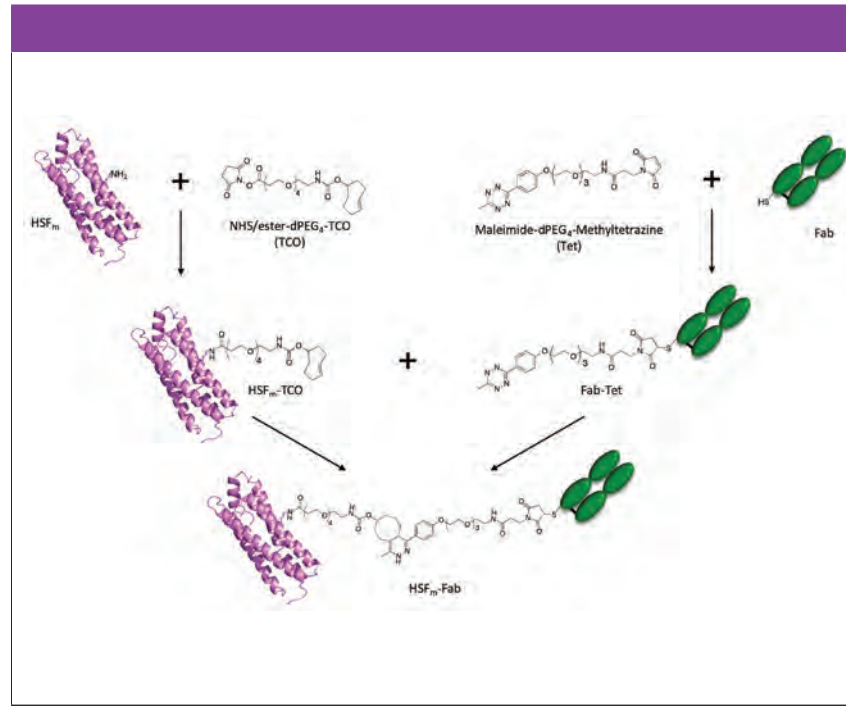

Figure 2: Schematic representation of reactions to form the HSF_m–Fab conjugate.

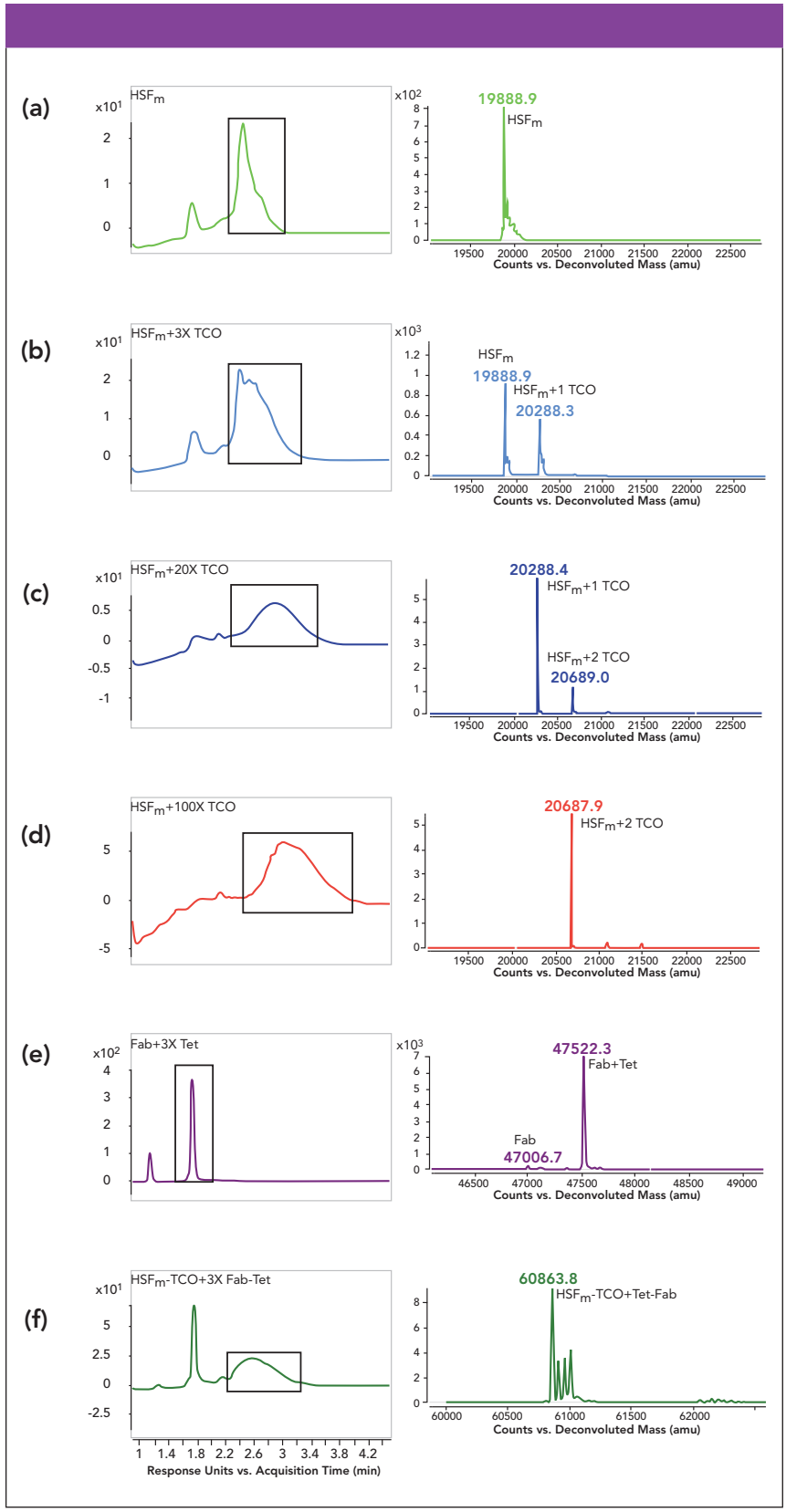

Figure 3: Reversed-phase-HPLC–MS of HSF-Fab conjugation reactions. Left panels show traces for absorbance (280 nm) where peaks being used for deconvolution are boxed in black, while right panels show corresponding deconvoluted masses (zoomed around masses of interest) for (a) HSF_m alone, reaction of HSF_m with NHS-TCO at a ratio of (b) 3-, (c) 20-, or (d) 100-fold excess TCO linker, (e) reaction of Fab with 3-fold excess of Mal-Tet linker and (f) SPAAC reaction of HSF_m-TCO with Tet-Fab.

Surprisingly, the addition of increasing amounts of the NHS-TCO to HSF resulted in decreased area (280 nm) and broadening of the HSF peak (Figure 3b–3d). Although it is not shown here, the decrease in signal was accompanied by suppression of ionization. One hypothesis to explain these findings pertains to the modified lysines. It is possible that the lysines implicated in the conjugation reaction make solvent contacts that are important for ionization, and the decrease in signal is related to increased conjugation of these lysines. Despite this issue, deconvoluted masses were still obtained, which allowed for characterization of the conjugation reaction.

As shown in the deconvoluted mass analysis in Figure 3b, a mixture of unreacted HSF_m and one NHS-TCO addition was detected at a reaction ratio of 3:1, while 1-2 additions were detected at a ratio of 20:1 (Figure 3c), and 2 additions were detected at a ratio of 100:1 (Figure 3d). Previously, Zeng and associates identified the presence of surface exposed labile lysines on HSF (25). They found that when a small NHS-alkyne molecule was conjugated to HSF, up to four small linkers were successfully added. However, when lysine reactivity was investigated using a bulky fluorescent probe (5-carboxyfluorescein *N*-hydroxysuccinimidyl ester) or when saturation of the multiple alkyne moieties was attempted using 3-azido-7-hydroxycoumarin, only one unit per monomer could be detected. In their study, the incomplete modification of HSF_m was attributed to steric hinderance since a 200-fold excess of each linker was being added in each reaction, which is consistent with the results reported here. Based on these combined findings, the 20:1 ratio was chosen because it yielded the highest conjugation efficiency of one linker per HSF_m.

In parallel with HSF-TCO synthesis, Fab containing a C-terminal Cys was conjugated under physiological conditions to a heterobifunctional maleimide (Mal), methyltetrazine (Tet), PEG_4 linker (Mal-Tet, Figure 2) (BroadPharm, BP-22436). The reactivity and lability of the Fab C-terminal Cys was previously reported (26); a 3-fold molar excess of the similar maleimide linkers is suffi-

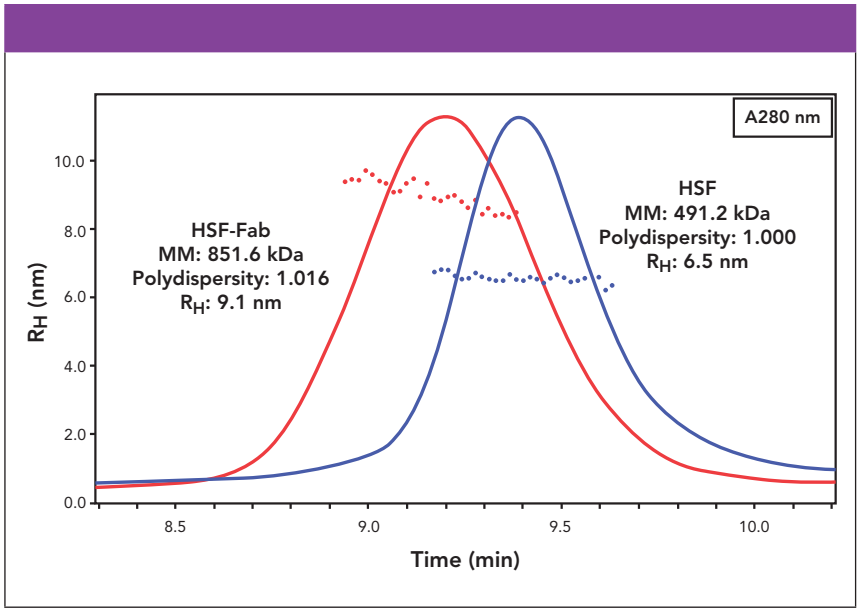

Figure 4: Hydrodynamic radius versus time: native analysis using SEC-MALS-QELS. Chromatogram of absorbance at 280 nm with R_H calculated from QELS overlaid across each peak. In addition, averaged molar mass (MM), polydispersity and R_H values for HSF and HSF-Fab conjugate are reported.

cient for complete reaction of the Fab Cys (2,27), which was confirmed for the Mal-Tet conjugation to generate the Tet-containing Fab (Fab-Tet) (Figure 3d). In the left panel, two peaks are present, where the peak with retention time around 1.3 min is Fab light chain that has dissociated under denaturing conditions because of a lack of disulfide pairing with the heavy chain, while the peak with retention time around 1.8 min corresponds to the properly assembled Fab. In the right panel, the predominant deconvoluted mass confirms close to complete modification of the Fab with Mal-Tet linker. Subsequent to activation of each molecule, unreacted linker was removed using SEC purification. (GE Healthcare, Superdex 200).

HSF-TCO was then conjugated to Tet-Fab (1:3) using strain-promoted azide-alkyne cycloaddition (SPAAC, Figure 2, 3e) (28–30). In the left panel of Figure 3e, two peaks are observed in the conjugation reaction, where the first peak corresponds to the unconjugated Fab-Tet (1.8 min retention time) and the second corresponds to the HSF-Fab conjugate (2.6 min retention time). In the right panel, the conjugate peak deconvoluted to a mass in-line with expectation. Additional peaks were also observed with an increase of 16–18 Da relative to calculated mass, which are likely water additions on HSF.

In addition to LC–MS analysis, the assembled HSF-Fab conjugate was characterized under native conditions by SEC-MALS-QELS (Figure 4). As shown in Figure 4, the SEC-MALS-QELS data support a well-behaved soluble conjugate, as confirmed by the symmetrical peak shape and lack of detectable aggregation, as well as an increase in molar mass (MM) and hydrodynamic radius (R_H) relative to the unconjugated HSF cage. Although the desired product was confirmed, the difference in MM between the HSF-TCO-Tet-Fab (851.6 kDa) and unconjugated HSF (491.2 kDa) suggests that not all 24 HSF_m-TCO subunits were saturated with Fab-Tet. The difference in MM between HSF-Fab and unconjugated HSF suggests an average of 7.7 Fabs per HSF cage, which is consistent with the steric hinderance issues observed by Zeng and associates (25). In that study, a 200-fold excess was used whereas in this work, only a 3-fold excess of Fab-Tet was added to the reaction. Perhaps with a greater excess of Fab-Tet, conjugation to all 24 subunits might be achieved. However, it is likely that there is too much steric crowding to allow for conjugation of 24 Fabs using this approach.

Materials and Methods

LC–MS analysis

Data was acquired as described previously (31), using an Agilent 1290 Infinity UPLC in tandem with an Agilent 6230 electrospray ionization time-of-flight (UPLC-ESI-TOF) mass spectrometer, operating in positive ion mode. For all gradients, mobile phase A consisted of 0.05% trifluoroacetic acid (TFA) in water while mobile phase B consisted of 0.05% TFA and 100% acetonitrile (Figure 1).

SEC-MALS/QELS Analysis of HSF and HSF-Fab Conjugate

Purity, molar mass (MM), and hydrodynamic radius (R_H) were determined using an Acclaim SEC-1000 analytical SEC column run on a Dionex UltiMate 3000 UPLC (Thermo Fisher Scientific), with isocratic elution in phosphate buffered saline (PBS) spiked with an additional 150 mM sodium chloride. In line with ultraviolet (UV) detection, a multi-angle laser light scattering (MALS) detector (Wyatt Instruments), was used to determine molar mass due to Brownian motion, as well as an attached quasi-elastic light scattering (QELS) detector (Wyatt Instruments), to capture fluctuations in intensity of laser light scattered, allowing diffusion coefficients to be measured. Assuming a spherical shape, the Stokes-Einstein relationship was used to calculate R_H from D.

Conclusions

This work demonstrates the design and production of a multivalent HSF-Fab conjugate, which presents many benefits as a nanotechnology platform. As a discrete entity, it is a simpler system relative to other delivery technologies such as large polydisperse polymers or liposomes. Moreover, since it is found ubiquitously in living organisms, it is inherently biocompatible, and is easily engineered (32–34). In a recombinant protein format, it has the potential to provide many quality attributes beneficial for downstream development and it is compatible with traditional protein purification techniques to take advantage of well-established manufacturing processes.

This strategy also provides flexibility in making bioconjugates. By using

FREE
CHROMACADEMY MEMBERSHIP

Agilent Technologies is offering five years complimentary access to CHROMacademy for all university students and staff.

CHROMacademy is an intuitive, comprehensive e-learning and trouble-shooting platform with more than 3,000 pages of content for HPLC, GC, sample preparation, and hyphenated techniques. No other online resource offers separation scientists more live streaming events, a knowledge base, practical solutions, and new technologies in one easy to navigate website.

Get your free five year membership worth US $1,995* by submitting the form at **www.chromacademy.com/agilent**.

* Five years free access to CHROMacademy only available to customers affiliated with an academic or research institution, conditions apply. A valid university e-mail address if required.

Agilent Technologies

bifunctional click chemistry linkers, virtually any two biomolecules can be conjugated together. Furthermore, the modular approach involving derivatization of each component separately, allows for control of purity at each step prior to clicking the partners together to form the final conjugate. In future work, we hope to explore longer PEG spacers with the goal of increasing conjugation efficiency, and engineering the HSF protein to install site-specific conjugation handles and avoid heterogeneous lysine conjugation.

References

(1) S. Bhaskar and S. Lim, *NPG Asia Mater* **9,** e371–e389 (2017). doi: 10.1038/am.2016.128.

(2) W. Shatz, P.E. Hass, N. Peer, M.T. Paluch, C. Blanchette, G. Han, W. Sandoval, A. Morando, K.M. Loyet, V. Bantseev, H. Booler, S. Crowell, A. Kamrath, J.M. Scheer, and R.F. Kelly, *PLoS ONE* 14:e0218613–20 (2019). doi: 10.1371/journal.pone.0218613.

(3) J.Y. Li, N. Paragas, R.M. Ned, A. Qiu, M. Viltard, T. Leete, I.R. Drexler, X. Chen, S. Sanna-Cherchi, F. Mohammed, D. Williams, C.S. Lin, K.M. Schmidt-Ott, N.C. Andrews, and J. Barasch, *Dev. Cell* **16**(1), 35–46 (2009). doi: 10.1016/j.devcel.2008.12.002.

(4) L. Li, C.J. Fang, J.C. Ryan, E.C. Niemi, J.A. Lebrón, P.J. Björkman, H. Arase, F.M. Torti, S.V. Torti, M.C. Nakamura, and W.E. Seaman, *PNAS* **107**(8), 3505–3510 (2010). doi: 10.1073/pnas.0913192107.

(5) S. Zhang, J. Zang, H. Chen, M. Li, C. Xu, and G. Zhao, *Small* **13,** 1701045–6 (2017). doi: 10.1002/smll.201701045.

(6) D. He and J. Marles-Wright, *N. Biotechnol.* **32,** 651–657 (2015). doi: 10.1016/j.nbt.2014.12.006.

(7) P.M. Harrison, *Biochem. Ed.* **14,** 154–162 (1986). doi: 10.1016/0307-4412(86)90203-7.

(8) P.M. Harrison and P. Arosio, *Biochim. Biophys. Acta* **1275,** 161–203 (1996). doi: 10.1016/0005-2728(96)00022-9.

(9) S. Ciambellotti, A. Pratesi, M. Severi, G. Ferraro, E. Alessio, A. Merlino, and L. Messori, *Dalton Trans.* **47,** 11429–11437 (2018). doi: 10.1039/C8DT00860D.

(10) J.M. Domínguez-Vera and F. Colacio, *Inorg. Chem.* **42,** 6983–6985 (2003). doi: 10.1021/ic034783b.

(11) X.T. Ji, L Huang, and H-Q. Huang, *J Proteomics* **75,** 3145–3157 (2012). doi: 10.1016/j.jprot.2012.03.013.

(12) Z. Yang, X. Wang, H. Diao, J. Zhang, H. Li, H. Sun, and Z. Guo, *Chem. Comm.* 3453–3455 (2007). doi: 10.1039/B705326F.

(13) N. Pontillo, F. Pane, L. Messori, A. Amoresano, and A. Merlino, *Chem. Comm.* **52,** 4136–4139 (2016). doi: 10.1039/C5CC10365G.

(14) N. Pontillo, G. Ferraro, J.R. Helliwell, A. Amoresano, and A. Merlino, *ACS Med. Chem. Lett.* **8,** 433–437 (2017). doi: 10.1021/acsmedchemlett.7b00025.

(15) R.Xing, X. Wang, C. Zhang, Y. Zhang, Q. Wang, Z. Yang, and Z. Guo, *J. Inorg. Biochem.* **103,** 1039–1044 (2009). doi: 10.1016/j.jinorgbio.2009.05.001.

(16) K. Fujita, Y. Tanaka, T. sho, S. Ozeki, S. Abe, T. Hikage, T. Kuchimaru, and S. Kizaka-Kondoh, *J. Am. Chem. Soc.* **136,** 16902–16908 (2014). doi: 10.1021/ja508938f.

(17) Y. Takezawa, P. Böckmann, N. sugi, Z. Wang, S. Abe, T. Murakami, T. Hikage, G. Erker, Y. Wantanabe, S. Kitagawa, and T. Ueno, *Dalton Trans.* **40,** 2190–2195 (2011). doi: 10.1039/c0dt00955e.

(18) D.M. Monti, G. Ferraro, G. Petruk, L. Maiore, F. Pane, A. Amoresano, M.A. Cinellu, and A. Merlino, *Dalton Trans.* **46,** 15354–15362. doi: 10.1039/C7DT02370G (2017).

(19) G. Ferraro, D.M. Monti, A. Amoresano, N. Pontillo, G. Petruk, F. Pane, M.A. Cinellu, and A. Merlino, *Chem. Comm.* **52,** 9518–9521. doi: 10.1039/C6CC02516A (2016).

(20) G. Ferraro, S. Ciambellotti, L. Messori, and A. Merlino, *Inorg. Chem.* **56,** 9064–9070. doi: 10.1021/acs.inorgchem.7b01072 (2017).

(21) L. Messori and A. Merlino, *Coord. Chem. Rev.* **315,** 67–89. doi: 10.1016/j.ccr.2016.01.010 (2016).

(22) T.G. Appleton, *Coord. Chem. Rev.* **166,** 313–359. doi: 10.1016/S0010-8545(97)00047-7 (1997).

(23) M. Kanekiyo, C-J. wei, H.M. Yassine, P.M. McTamney, J.C. Boyington, J.R.R. Whittle, S.S. Rao, W-P. Kong, L. Wang, and G.J. Nabel, *Nature* **499,** 102–106 (2013). doi: 10.1038/nature12202.

(24) J.M. Hooker, A. Datta, M. Botta, K.N. Raymond, and M.B. Francis, *Nano. Lett.* **7,** 2207–2210 (2007). doi: 10.1021/nl070512c.

(25) Q. Zeng, R. Reuther, J. Oxsher, and Q. Wang, *Bioorg. Chem.* **36,** 255–260 (2008). doi: 10.1016/j.bioorg.2008.06.001.

(26) S. Jevševar, M. Kusterle, and M. Kenig, in *Site-Specific Protein Labeling,* P. Chames, Ed. (Humana Press, Totowa, New Jersey, 2012), pp 233–246.

(27) W. Shatz, P.E. Hass, M. Mathieu, H.S. Kim, K. leach, M. Zhou, Y. Crawford, A. Shen, K. wang, D.P. Chang, M. Maia, S.R. Crowell, L. Dickmann, J.M. Scheer, and R.F. Kelley, *Mol. Pharm.* **13**(9), 2996–3003 (2016). doi: 10.1021/acs.molpharmaceut.6b00345.

(28) N.J. Agard, J.A. Prescher, and C.R. Bertozzi, *J. Am. Chem. Soc.* **126,** 15046–15047 (2004). doi: 10.1021/ja044996f.

(29) J.M. Baskin, J.A. Prescher, S.T. laughlin, N.J. Agard, P.V> Chang, I.A. Miller, A. Lo, J.A. Codelli, and C.R. Bertozzi, *PNAS* **104,** 16793–16797 (2007). doi: 10.1073/pnas.0707090104.

(30) J. Dommerholt , F.P.J.T. Rutjes, and F.L. van Delft, *Top Curr. Chem. (Cham)* **374,** 16–20 (2016). doi: 10.1007/s41061-016-0016-4.

(31) J. Zarzar, W. Shatz, N. Peer, R. Taing, B. McGarry, Y. Liu, D.G. Greene, and I.E. Zarraga, *Biophys. Chem.* **236,** 22–30 (2017). doi: 10.1016/j.bpc.2017.10.003.

(32) T. Treffry, P.M. Harrison, A. Luzzago, and G. Cesareni, *FEBS Letters* **247,** 268–272 (1989).

(33) P. Santambrogio, S. Levi, A. Cozzi, E. Rovida, A. Albertini, and P. Arosio, *J. Biol. Chem.* **268,** 12744–12748 (1993).

(34) P. Rucker, F.M. Torti, and S.V. Torti, *Protein Eng., Des. Sel.* **10**(8) 967–973 (1997). doi: org/10.1093/protein/10.8.967.

Whitney Shatz, Remo Perozzo and **Yogeshvar N. Kalia** are with the School of Pharmaceutical Sciences at the University of Geneva, in Geneva, Switzerland. **Shatz, Craig Blanchette, Patrick Holder,** and **Robert F. Kelley** are with Genentech, in South San Francisco, California. Direct correspondence to: shatz.whitney@gene.com

Utilizing Multidimensional LC–MS for Hydroxyl Radical Footprinting Analysis

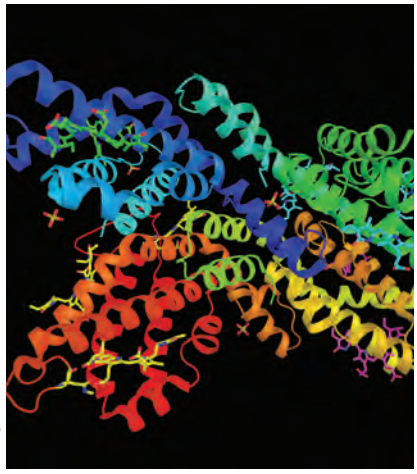

Image credit: ibreakstock/stock.adobe.com

Research tools that can decipher protein–protein interactions and binding interface contact points can aid in the successful development of biotherapeutics. Hydroxyl radical footprinting–mass spectrometry (HRF-MS) technologies are being developed as tools for deciphering protein–protein interactions. We have demonstrated the utility of using fast photochemical oxidation of proteins (FPOP) as an HRF-MS technology for biotherapeutic protein structural characterization and analysis of protein–protein interfaces; monoclonal antibody (mAb) epitope mapping has also been demonstrated using this technique. However, the postlabeling workflow that utilizes offline protein digestion and liquid chromatography–tandem mass spectrometry (LC–MS/MS) analysis is labor intensive and time consuming, and has significant sample consumption. In the present work, we demonstrate the potential of multidimensional online peptide mapping analysis (reduction, tryptic digestion, and separation) as a strategy for improving our postlabeling workflow for protein–protein interactions. The proof-of-concept studies were performed using a Fab antibody fragment and its antigen binding partner.

Julien Camperi,* Arthur John Schick,* Davy Guillarme, and Aaron T. Wecksler*

*Authors contributed equally to this work.

Monoclonal antibody (mAb) structural characterization and their epitope mapping are both important aspects of biotherapeutic discovery to further understand structure-function relationships, mechanisms of action, and antibody–antigen binding interactions (1). The most commonly used techniques for epitope mapping are nuclear magnetic resonance (NMR) and X-ray crystallography, which provide high-resolution information on binding interactions at the atomic level (2,3). However, these techniques may have limited biological relevance, most notably for the analysis of structure and dynamics of proteins in conformation states of interest, and are especially challenging for large, complex proteins. On the other hand, spectroscopy-based approaches such as Fourier transform–infrared spectroscopy (FT-IR) (4), analytical ultracentrifugation (AUC) (5), and fluorescence spectroscopy (6) can be used for mAb structural characterization, providing residue-specific information or high-throughput analysis, or both. However, these methods are not suitable for localizing specific areas or regions of structural change in the proteins, and are generally considered as low resolution techniques.

Alternatively, footprinting based on liquid chromatography–mass spectrometry (LC–MS) has recently emerged as a powerful approach for the structural characterization and elucidation of protein–protein interactions (7,8). These techniques are considered bottom-up MS approaches to protein analysis in which proteins are labeled, subsequently digested, and then analyzed by liquid chromatography–tandem mass spectrometry (LC–MS/MS), providing information on solvent accessibility for specific chains in the protein structure. Information on the solvent accessibility of the peptides can be encoded onto the peptides by means of either reversible (hydrogen/deuterium exchange [HDX]) or irreversible (hydroxyl radicals) chemical probes (1).

Table I: Offline versus online workflows for the peptide mapping analysis of a Fab molecule. The sequence coverages (Seq. coverage), relative standard deviation (RSD) values of the retention times (tr) and areas, and the analysis times are given.

	Digestion step	LC–MS/MS	Analysis Time
Off-line workflow	Seq. coverage, Fab ≈97%	RSD_{tr} (n = 3): 0.25–0.32% RSD_{area} (n =3): 1.62–10.75%	12–13 h
On-line workflow	Seq. coverage, Fab ≈88%	RSD_{tr} (n = 3): 0.16–0.76% RSD_{area} (n =3): 3.73–8.12%	**100 min**

Another growing technology in the epitope mapping field is hydroxyl radical footprinting–mass spectrometry (HRF-MS) (9–11). HRF-MS uses a high powered laser to photodissociate hydrogen peroxide into hydroxyl radicals, enabling the covalent and irreversible labeling of protein residues. The addition of hydroxyl groups to protein side chains induces a +16 mass shift, easily detectable by tandem MS analysis. Because of the irreversible labeling reaction, no extra care is needed for the postlabeling workflow. However, the conventional approach for the postlabeling workflow involves time-consuming offline procedures, with reduction and alkylation of the protein and buffer exchange, followed by an offline tryptic digestion before injection onto an LC–MS instrument. In addition, the tryptic digestion in solution also suffers from a number of drawbacks such as low efficiency and autodigestion of the enzyme (12).

Recently, fast, online, and automated multidimensional LC workflows have been developed on commercial ultrahigh-pressure liquid chromatography (UHPLC) systems for the reduction and digestion of proteins, bypassing the offline manual sample pretreatment reduction and digestion of mAbs (13). The use of these instruments for automated and fast digestion under high pressure with immobilized trypsin cartridges significantly reduces the digestion times compared to the standard offline approach (minutes vs. hours). Using the multidimensional LC–MS approach (automated online reduction, digestion, and separation) for the postlabeling HRF-MS workflow can significantly reduce sample handling and operator time compared to standard offline procedures. In this study, we explore this possibility of using a multidimensional LC workflow to analyze the known paratope (the complementarity determining region, [CDR]) map of a monoclonal Fab fragment against its antigen, and compare the results against the conventional offline procedure.

Experimental Method

Reagents and Sample Preparation

Millipore Sigma provided the hydrogen peroxide (30%), dithiothreitol (DTT), sodium iodoacetate (IAA), and all MS-grade solvents (2-propanol and acetonitrile). Tris(hydroxymethyl) aminomethane (TRIS) base, potassium phosphate monobasic, potassium phosphate dibasic, potassium chloride, MS-grade formic acid (FA) and trifluoroacetic acid (TFA) were all purchased from Sigma-Aldrich. Calcium chloride dihydrate and sodium chloride were obtained from BeanTown Chemicals. Water was obtained from a Milli-Q purification system from Millipore. MS-grade water, 0.1% FA in water, 0.1% FA in acetonitrile and tris(2-carboxyethyl) phosphine hydrochloride (TCEP-HCl) were all purchased from Thermo Fisher Scientific.

The antigen and the Fab were produced in *Escherichia coli* cells and prepared for labeling by size-exclusion chromatography. Samples were purified and buffer exchanged using a TSKgel UP-SW3000 column (4.6-mm I.D. x 30 cm, 2-µm) purchased from Tosoh Bioscience and a 0.2 M potassium phosphate, 0.25 M potassium chloride, pH 6.2 buffer. Samples were collected off the column and diluted to approximately 2 mg/mL for labeling. The antigen–Fab complex was created by mixing the components at a 1:2 antigen–Fab ratio.

Hydroxyl Radical Labeling Procedure

Samples were subjected to labeling as previously described (14). Briefly, a high power laser was focused on a glass capillary used to irradiate the sample. Two syringes, one containing the protein samples (Fab or antigen–Fab complex) combined with arginine (used to help control the amount of hydroxyl labeling), and the other syringe (containing hydrogen peroxide), converged on a T-mixer just before the point of laser irradiation. This T-mixer allowed the solution to mix at a 2:1 (protein:hydrogen peroxide) volume ratio. After irradiation, the samples are delivered in-line to a sample tube containing methionine and catalase to quench the labeling reaction.

Standard Off-line Peptide Mapping Approach

Hydroxyl radical labeled protein samples were digested as previously described (14). Briefly, the proteins were reduced with guanidine HCl (6 M) and DTT (10 mM, 45 °C for 10 min), and alkylated with IAA (25 mM, at room temperature for 5 min), and quenched with DTT (50 mM, room temperature). The resulting samples were then desalted using NAP-5 columns (GE Healthcare), digested with trypsin (5 µg, 37 °C, overnight), and quenched with 100% of FA.

Tryptic peptides (10 µg) separation was performed using a Waters H-Class UPLC system with a Waters Acquity UPLC CSH130 C-18 column (1.7-µm, 2.1 mm × 150 mm). The flow rate was fixed at 0.3 mL/min and the column temperature at 77 °C. Mobile phases consisted of 0.1% FA in water (A) and acetonitrile (B). The gradient conditions consisted of 0 to 35% B in 42 min. The MS analysis was carried out with a ThermoFisher QExactive Orbitrap MS operating in positive mode, performing MS^2 scans on the top-10 most abundant peaks in data-dependent acquisition mode in the *m/z* range 350–2000 at a resolving power of 35,000. MS data treatment was performed using Byonic and Byologic Footprint Software Suites (Protein Metrics, Inc.) for peak identification and quantitation of percent modification for each peptide, respectively. All samples were analyzed in triplicate.

On-line Peptide Mapping Analysis

Instrument

All online peptide mapping analyses were carried out on a biocompatible ThermoScientific Dionex UltiMate 3000 Rapid Separation (RS) system. It is composed of two RS dual pump modules, each containing two ternary pumps, two thermo-

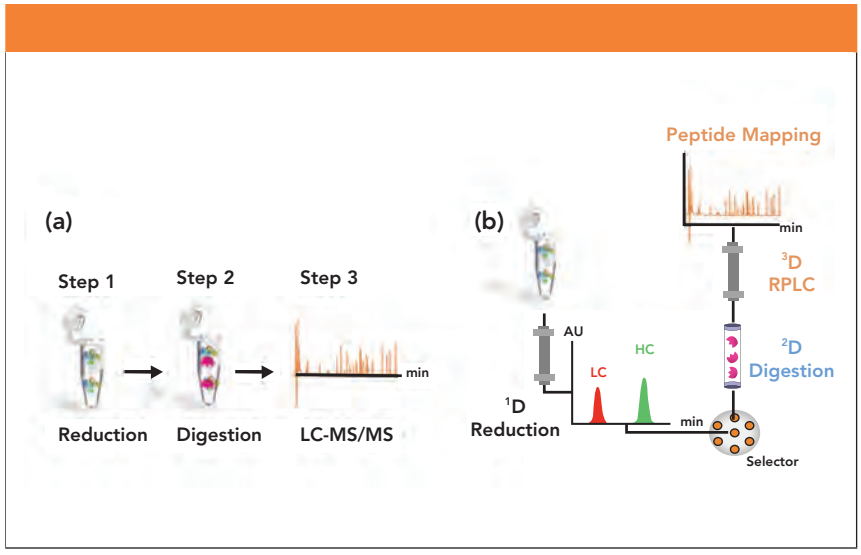

Figure 1: Schematic representation of (a) conventional offline and (b) online peptide mapping (reduction-reversed-phase LC x tryptic-digestion x reversed-phase LC–MS) workflows for hydroxyl radical footprinting analysis.

static RS column compartments, and an RS auto sampler. The multidimensional LC setup was coupled to a Q Exactive Orbitrap MS. For multidimensional LC–MS analysis, the same MS parameters for the standard offline peptide mapping approach were used.

1st Dimension (^{1}D): On-column Reduction

Hydroxyl radical labeled proteins were first loaded and reduced on column using the BioResolve RP mAb Polyphenyl column (2.1-mm I.D. x 50 mm, 2.7-µm, 450 Å) purchased from Waters. Mobile phases A and B contained 0.1% FA and 0.05% TFA in water and acetonitrile, respectively. Mobile phase C contained the TCEP reducing agent at 25 mM in acidified water (pH 4.5). The valve located between the second- and third-dimension columns was switched at 20 min when the elution starts to divert the reduced proteins to the third dimension trypsin cartridge. Supplemental Table S1 lists the gradient and valve details.

2nd Dimension (^{2}D): Tryptic Digestion in Flow-Through Mode

The Poroszyme immobilized trypsin cartridge (2.1-mm I.D. x 30 mm), supplied by Thermo Fisher, was equilibrated from 0 to 20 min, then set in-line with the ^{1}D and ^{3}D reversed-phase LC columns from 20 to 50 min, for the online digestion and subsequent trapping of the peptides on the ^{3}D reversed-phase LC column. Digestion buffer was composed of 10 mM calcium chloride and 50 mM TRIS pH 8.0, whereas a 2-propanol/acetonitrile (70:30, *v/v*) mixture was used to wash the trypsin cartridge after each cycle.

3rd Dimension (^{3}D): Peptide Mapping Analysis

The trapped peptides from 20 to 50 min were then eluted between 50 min and 100 min from an XSelect CSH C18 column (2.1-mm I.D. x 150 mm, 3.5-µm, 450 Å) supplied by Waters. MS grade mobile phases A and B were composed of 0.1% FA in water and acetonitrile, respectively. Table S1 lists the gradient and valve details.

Results and Discussion

Off-line Versus On-line Workflows

Figure 1 shows the two workflows for the (a) conventional offline and (b) online peptide mapping approaches. With the online peptide mapping workflow, the Fab sample was injected onto the ^{1}D reversed-phase LC column, where it was subsequently trapped at the head of the column. For the reduction of the Fab into reduced subunits (heavy chain and light chain), a 25 mM TCEP solution in acidified water (pH 4.5) was used. The reduced Fab chains eluted from the ^{2}D column and were then digested online on the immobilized trypsin cartridge, prior to their separation on the ^{3}D reversed-phase LC coupled to MS.

The precision of the online multidimensional LC digestion workflow was compared to the standard offline procedure to assess whether there were differences between the workflows and whether the multidimensional LC approach could be used for hydroxyl radical footprinting analysis. A Fab molecule was selected and three consecutive injections were performed on the online system and compared with a conventional offline procedure (Table I). A sequence coverage of 88% using the online workflow, compared to the offline value of 97%, was achieved, and the sequence coverage remained consistent for each experiment. The difference in sequence coverage results from the absence of a single peptide with the online approach, which is discussed in the next section. The repeatability of the online peptide mapping method was then assessed by

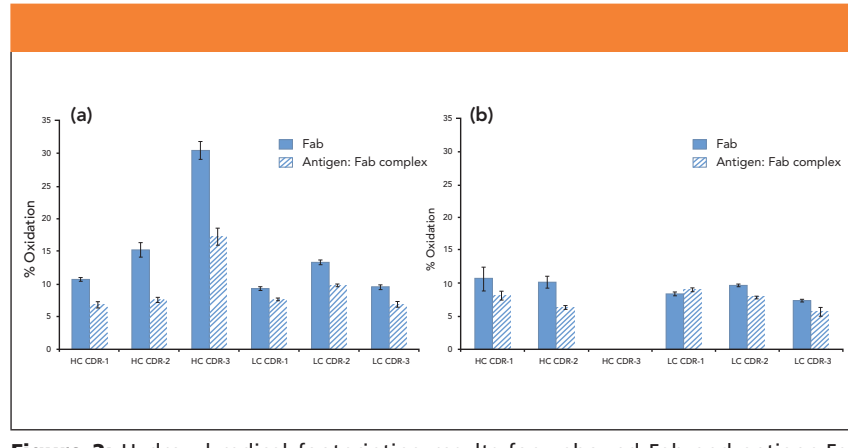

Figure 2: Hydroxyl radical footprinting results for unbound Fab and antigen:Fab complex for (a) offline HRS-MS procedure, and (b) online HRS-MS procedure. HRF analysis was completed on the Fab heavy and light chain CDR-containing peptides.

performing triplicate analysis. For this purpose, four unmodified peptides in common with the offline approach were selected and compared according to their retention times and peak areas. As shown in Table I, the results demonstrated a repeatability of the online analysis with relative standard deviation (RSD) values lower than 0.8% and 8.2% for the retention times and peaks areas, respectively.

The leading advantage of the multidimensional LC online peptide mapping approach is the short analysis time with a turnaround of 100 min compared to the conventional offline procedure, which typically requires several hours (Table I). The decrease in analysis time is achieved by the automation of all the labor-intensive and manual sample preparation steps associated with the conventional offline approach, including reduction/alkylation, desalting, digestion, and buffer exchange. Another advantage of the online approach is the low amount of sample required (10 µg per injection for the online peptide mapping analysis, compared to 100 µg typically required for the offline digestion), resulting from the low efficiency of the tryptic digestion in solution.

Off-line versus On-line HRF-MS Results

The amount of oxidation that occurs during HRF labeling for a given region of a protein is proportional to the solvent accessibility of the region. Comparing the oxidation of Fab peptides in the unbound and bound antigen–Fab complex state allows for paratope mapping of the antigen–Fab interaction, where the regions showing a decrease in oxidation in the bound state are possible binding paratopes. The CDR-containing peptides, the known paratopes in this interaction, were analyzed for both offline and online digested samples to understand if the online digestion method could be used for the paratope mapping analysis from HRF labeling.

Data analysis was conducted similarly between the offline and online samples (see experimental section). The offline peptide mapping samples indicated a decrease in oxidation (possible binding paratope) in the antigen–Fab complex sample compared to the Fab sample in peptides containing the CDRs (Figure 2). The multidimensional LC online peptide mapping results also indicated a decrease in oxidation in most of the CDR peptides detected with the offline procedure (4 out of 6 CDR-containing peptides), showing confidence in the use of the online automated approach for the HRF-MS paratope mapping workflow. Some of the differences between the online and offline results include the heavy chain CDR 3 peptide not being detected by the online digestion procedure, and the light chain CDR 1 peptide showing no significant difference in oxidation between Fab and antigen–Fab complex after online digestion. These differences are most likely attributable to the elution gradients in multidimensional LC–MS, where the very hydrophobic heavy chain CDR 3 peptide is retained on the ^{3}D reversed-phase LC column. Further method optimization of the online workflow is needed to increase the sequence coverage and recover the CDR 3 peptide. However, overall this proof of concept study shows that there is general agreement between the results generated with the offline and online digestion procedures, showing that HRF-MS analysis can be performed using the multidimensional LC online digestion procedure to make data acquisition faster and easier.

Conclusion

In this work, we introduced an innovative multidimensional LC–MS setup for a fast (100 min per run), automated, and online peptide mapping workflow for postlabeling HRF-MS epitope mapping analysis. Although the heavy chain CDR 3 peptide was not detected by the online approach, paratope mapping results were generally similar between the online and offline workflows. From these results, we can conclude that with further optimization, the online multidimensional LC system can be used for hydroxyl radical footprinting analysis to reduce the postlabeling workflow time from >10 h to 100 min.

Acknowledgments

The authors acknowledge Matt Kalo and Jennifer Rea from Genentech (South San Francisco, California, USA) for their support.

Supplemental Information

A supplemental table, showing on-column reduction and subsequent separation of reduced proteins, followed by on-line tryptic digestion and peptide mapping analysis, can be found online in the issue archive where this article appears.

References

(1) K. F. M. Opuni et al., *Mass Spectrom. Rev.* **37**(2), 229–241 (2018).
(2) O. Carugo and P. Argos, *Protein Sci.* **6**(10), 2261–2263 (2008).
(3) Q. Xu et al., *J. Mol. Biol.* **381**(2), 487–507 (2008).
(4) J. Kong and S. Yu, *Acta Biochim. Biophys. Sin.* **39**(8), 549–559 (2007).
(5) J. T. Pelton and L. R. McLean, *Anal. Biochem.* **277**(2), 167–176 (2000).
(6) O. Tcherkasskaya, V. E. Bychkova, V. N. Uversky, and A. M. Gronenborn, *J. Biol. Chem.* **275**(46), 36285–36294 (2000).
(7) A. Artigues et al., in *Modern Proteomics–Sample Preparation, Analysis, and Practical Applications*, H. Mirzaei and M. Carrasco, Eds. (Springer International Publishing, Cham, 2016). pp. 919, 397–431.
(8) H. Zhang, W. Cui, and M. L. Gross, *FEBS Lett.* **588**(2), 308–317 (2014).
(9) A. T. Wecksler, M. S. Kalo, and G. Deperalta, *J. Am. Soc. Mass Spectrom.* **26**(12), 2077–2080 (2015).
(10) G. Deperalta et al., *mAbs* **5**(1), 86–101 (2013).
(11) J.G. Kiselar and M.R. Chance, J. *Mass Spectrom.* 45(12), 1373–1382 (2010).
(12) S. Perchepied et al., *Talanta* **206,** 120171 (2020).
(13) C. Gstöttner et al., *Anal. Chem.* **90**(3), 2119–2125 (2018).
(14) M. Lin, D. Krawitz, M. D. Callahan, G. Deperalta, and A. T. Wecksler, *J. Am. Soc. Mass Spectrom.* **29**(5), 961–971 (2018).

Julien Camperi, Arthur John Schick, and Aaron T. Wecksler are with the Protein Analytical Chemistry group at Genentech Inc., in South San Francisco, California. ***Davy Guillarme*** is with the School of Pharmaceutical Sciences at the University of Geneva, in Switzerland. Direct correspondence to: wecksler.aaron@gene.com

Development of a Size-Exclusion Chromatography Method to Characterize a Multimeric PEG–Protein Conjugate

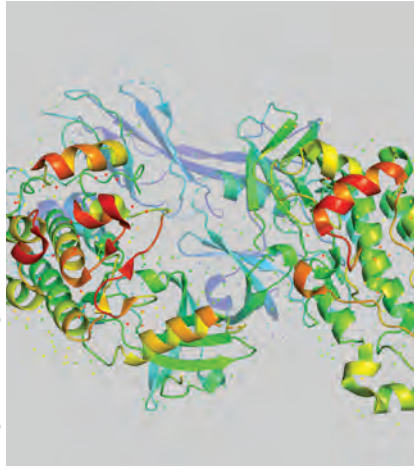

Image credit: sergent/stock.adobe.com

Conjugation of poly(ethylene glycol) (PEG) to therapeutic molecules is a widely used technique to increase in vivo half-life of therapeutics. A multimeric PEG–protein conjugate, which contains eight antigen-binding fragments (Fabs) conjugated to an 8-arm PEG core, was developed as a therapeutic candidate for age-related macular degeneration (AMD). The increased molecular size of the conjugate, compared to the Fab alone, produces a significant longer half-life, and requires less frequent intravitreal (ITV) injections, which can greatly benefit the patient. Due to the major impact that molecular size has on in vitreous half-life, it is crucial to have an analytical method to monitor the size attribute of the conjugate. Here we report a simple and robust size-exclusion chromatography (SEC) method that was developed for the conjugate. A wide range of size variants of the conjugate, ranging from 50 kDa to >1000 kDa, can be resolved and quantitated. The method was evaluated for precision, accuracy, linearity, and robustness, and was deemed suitable for routine use in product quality control.

Lu Dai, Joseph Elich, and Fred Jacobson

Poly(ethylene glycol) (PEG) is a water-soluble, nontoxic, non-antigenic, biocompatible polymer that has long been utilized in the fields of biotechnology and pharmacology (1,2). PEGylation of peptides, proteins, and other therapeutic entities can improve their pharmacological properties by increasing water solubility (3), reducing immunogenicity (4), and increasing half-life (5,6). These advantages have made PEGylation one of the most attractive and prevalent techniques in drug delivery. More than 10 PEGylated drugs have been approved by the FDA since the 1990s, and new PEGylated agents continue to enter and expand clinical pipelines (7).

In PEGylation, linear PEGs are the simplest and most commonly used conjugate agents. Most of the approved PEGylated drugs are conjugates with one or multiple linear PEG chains, such as PEGylated bovine adenosine deaminase (Adagen), PEGylated L-asparaginase (Oncaspar), and PEGylated α-interferon (PEG-INTRON) (8). On the other hand, novel PEG geometries with varied branching, chain length, and polydispersity have recently been utilized more in drug PEGylation, providing improved pharmacological properties compared to linear PEGs. One example is multi-armed PEG. With a star-like structure carrying multiple conjugation sites, it is shown to increase the active ingredient ratio, while simultaneously offering advantages of increased half-life and reduced immunogenicity (9).

A novel multi-armed PEG-protein conjugate, which contains eight antigen-binding fragments (Fabs) conjugated to an 8-arm PEG core, was developed as a drug candidate for age-related macular degeneration (AMD) (10). With an increased hydrodynamic radius (R_H), the multimeric PEG–Fab conjugate produces a significant longer vitreal half-life than Fab alone. The large Fab:PEG ratio also enables more protein delivery compared to the con-

CANNABIS science and technology

Connect with us on Social Media

Join your colleagues in conversation and stay up-to-date on breaking news, research, and trends associated with the legal cannabis industry. "Like" and follow us on Facebook, LinkedIn, Twitter, and Instagram today!

facebook.com/CannSciTech

linkedin.com/groups/12090641

twitter.com/CannabisSciTech

instagram.com/CannabisScienceTechnology

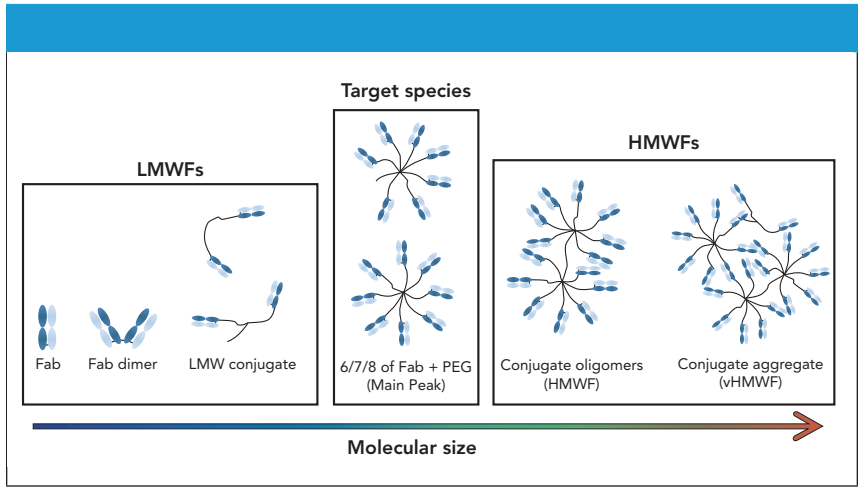

Figure 1: Schematic of the expected size variants in the PEG–Fab conjugate sample.

jugate with low Fab:PEG ratio. These improved properties make the multimeric PEG–Fab conjugate a promising ocular therapeutic with increased exposure and less dosing frequency, which can greatly benefit the patients.

As part of drug development, reliable qualitative and quantitative methods are required for product characterization and quality control. For the PEG–Fab conjugate, it is crucial to have an analytical method to monitor the size attribute, which is proven to be a key determinant of vitreal half-life (6). Due to the large molecular size of the PEG–Fab conjugate target form, a product specific size-exclusion chromatography (SEC) with optimal resolution for all the product-related size variants was developed. A qualification study was further conducted to assess the method for specificity, precision, accuracy, linearity, and robustness.

Experimental

Reagents and Samples

Sodium phosphate dibasic, sodium phosphate monobasic, sodium chloride, L-arginine monohydrochloride, sodium azide, and sodium sulfate were purchased from Sigma-Aldrich. Isopropyl alcohol was purchased from EMD Millipore. Hydrochloric acid standard solution (5.996 mol/L) and sodium hydroxide solution (5.0 mol/L) were purchased from Fluka. Water was obtained with a Milli-Q Purification system from Millipore.

Samples

PEG–protein conjugate used in this study consists of eight Fabs conjugated to an 8-arm 40 kDa PEG core. The Fab protein was expressed in *E. coli* and it contains an unpaired hinge cysteine on the C-terminal of the heavy chain. The PEG molecule used in the conjugation is an 8-arm PEG with a maleimide group on the end of each arm. The PEG–Fab conjugate was formed via the covalent bondage between the maleimide of the PEG and the C-termini cysteine of the Fab.

The stock solution of the PEG–Fab conjugate had a Fab concentration of 50 mg/mL and was diluted to the target concentration, 5 mg/mL, with 5 mM histidine hydrochloride, pH 5.5 buffer before the injection.

Instrumentation and Chromatographic Conditions

All measurements were performed using a Waters Alliance HPLC with multiple wavelength detector (MWD) or diode array detector (DAD). A Wyatt µDAWN multi-angle light scattering (MALS) detector and a Wyatt Optilab UT-rEX differential refractive

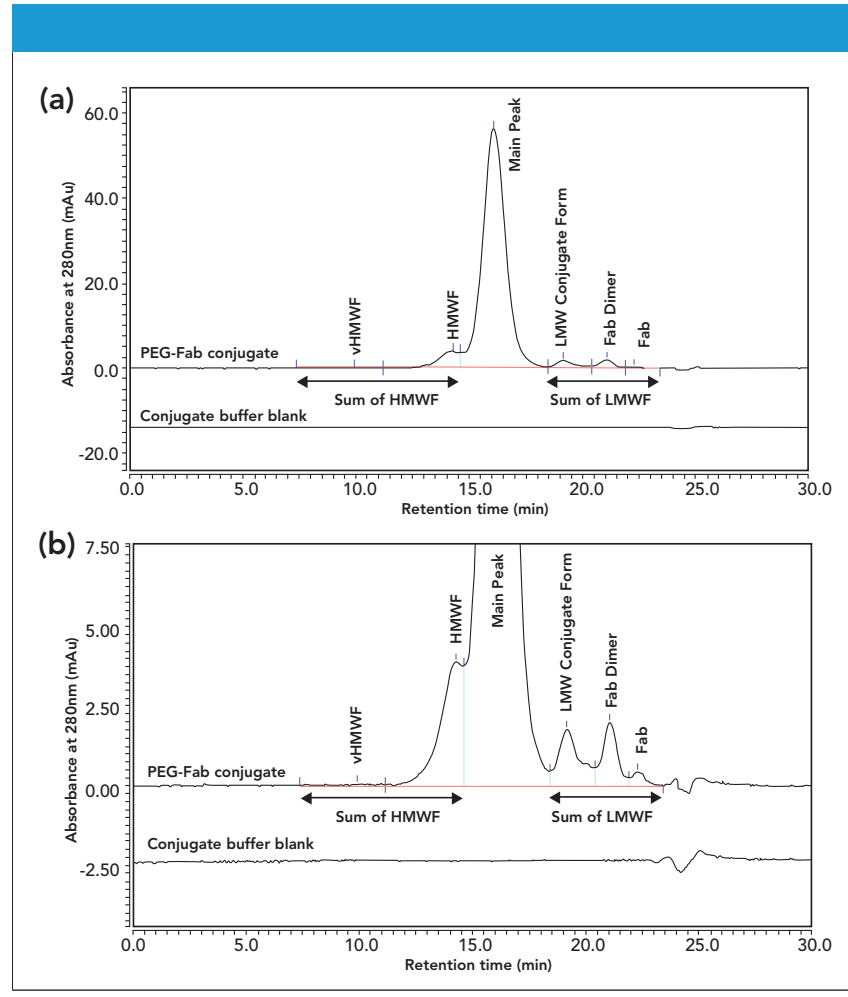

Figure 2: (a) Full-scale, and (b) enlarged representative SEC chromatogram of the PEG–Fab conjugate using a Tosoh TSKgel G4000SWXL column.

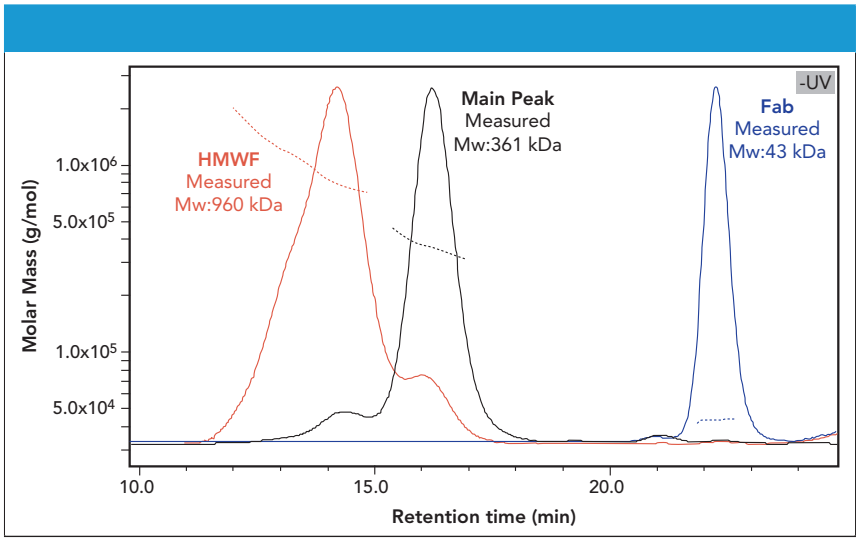

Figure 3: SEC-MALS for enriched HMWF sample, PEG–Fab conjugate and Fab, with measured molecular weight across ultraviolet (UV) trace demonstrates the effective separation of the size variants.

index (dRI) detector were coupled to the HPLC sequentially to measure the molecular weight of the eluting peaks.

Tosoh TSKgel G4000SWXL column (7.8 mm x 300 mm, 8-µm) was purchased from Tosoh Bioscience LLC. All separations were in isocratic mode at a flow rate of 0.5 mL/min and with a ultraviolet (UV) detection at 280 nm. The optimized mobile phase consisted of 100 mM sodium phosphate, 300 mM arginine, pH 6.2 with 10% IPA. Injection volume was 10 µL with a Fab concentration of 5.0 mg/mL.

Results and Discussion

Method Development

Column Screening

Consisting of 8 Fabs of 47 kDa and a PEG core of 40 kDa, the theoretical molecular weight (MW) of the PEG–Fab conjugate is 416 kDa. Due to conjugate aggregation, heterogeneity of PEG core, incomplete conjugation, and dimerization of Fab, many size variants can form. As shown in Figure 1, conjugate with 6, 7, or 8 Fabs are the target species. Potential low molecular weight forms (LMWFs) include free Fab, Fab dimer, and LMW conjugate that consists of a low number (2 or 3) of Fab and LMW PEG. Conjugate oligomer and aggregate can form as high molecular weight form (HMWF) and very high molecular weight form (vHMWF). Effective monitoring of these variants requires a SEC method capable of resolving both LMWFs and HMWFs with a range of MW from ~50 kDa to over 1000 kDa.

After screening a few SEC columns with the desired mass range (data not shown), Tosoh TSKgel G4000SWXL column (7.8 mm x 300 mm, 8-µm) showed the best resolution of HMWFs, main peak and various LMWFs and was selected for further optimization. A representative chromatogram of the PEG–Fab conjugate obtained with the Tosoh TSKgel G4000SWXL column is shown in Figure 2. To confirm the identity of the SEC peaks, enriched HMWF and Fab samples were run together with the conjugate sample by SEC-MALS (Figure 3). Average molecular weight of each peak was determined and showed agreement with the theoretical values, confirming the effective separation of size variants by the Tosoh TSKgel G4000SWXL column.

Mobile Phase Screening

The SEC mobile phase used during the initial column screening experiment was 20 mM sodium phosphate, 300 mM sodium chloride, pH 6.2. However, during an extended method evaluation, the repeatability of the results for the same sample on different columns and during different runs was not acceptable. More specifically, in three testing runs on two columns of different lots, the relative peak area of the sum of HMWF region has a %RSD of 29.6% and the relative peak area of the sum of LMWF has a %RSD of 40.0%. Inconsistent SEC profiles can often appear as a result of nonspecific interactions between the sample and the column resin. Sodium chloride is commonly used to reduce the electrostatic interaction between the sample and resin surface, but it cannot suppress the hydrophobic interaction. On

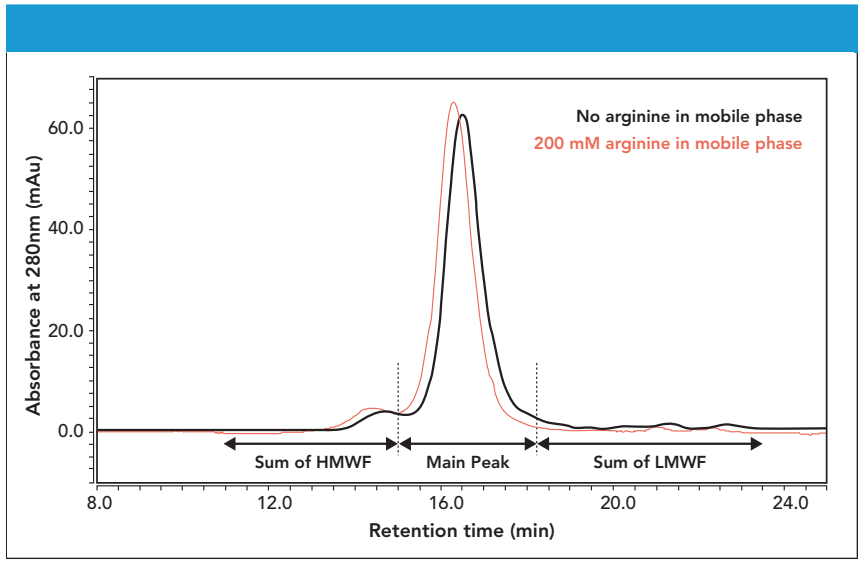

Figure 4: Comparison of chromatograms with and without 200 mM arginine in the mobile phase (20 mM sodium phosphate, 300 mM NaCl, pH 6.2).

the other hand, arginine is typically added to the mobile phase to suppress the hydrophobic interaction between sample and resin without aggregating or dissociating proteins (11). To assess the effect of arginine, the PEG–Fab conjugate sample was analyzed by SEC with and without 200 mM arginine in the mobile phase (Figure 4). With the presence of arginine, all peaks eluted earlier and the total peak area increased, proving the nonspecific interactions were reduced between the sample and the column resin.

After screening different arginine concentrations in the mobile phase, 300 mM arginine was selected because it resulted in the lowest peak retention time and the largest peak area, demonstrating minimal sample-resin interactions. In addition, 10% (*v/v*) IPA was added to the mobile phase as a microbial inhibitor after bacterial growth observed in the mobile phase during storage at ambient temperature. This extended the mobile phase storage time to 2 weeks without significant impact on the SEC separation. The optimized mobile phase was 100 mM sodium phosphate, 300 mM arginine, pH 6.2 with 10% IPA.

Optimization of Other SEC Parameters

In all modes of chromatography, high sample load tends to lead to higher sensitivity but generally reduces the resolution. For this method, injection volume was optimized to 10 µL with a Fab concentration of 5.0 mg/mL as a compromise between sensitivity and resolution.

The impact of column temperature on method performance was also tested by changing the column temperature from 24 °C to 30 °C. Higher column temperature resulted in lower column pressure and sharper peaks compared to the lower temperature. A column temperature of 28 °C was selected to achieve better performance while accommodating the column's recommended maximum temperature of 30 °C.

Method Qualification

After the SEC conditions were optimized, a method qualification was conducted to assess the specificity, stability indicating property, precision, accuracy, and linearity. Method robustness was also evaluated through a design of experiment (DOE) study.

Specificity and Stability Indicating Property

To assess the specificity and stability indicating property, the conjugate buffer blank, PEG–Fab conjugate (t0), and the thermally stressed conjugate sample (4 weeks, 40 °C) were run with the optimized conditions. As shown in Figure 5, there was no significant interference from the matrix components for the quantification of the size variants, demonstrating a suitable specificity of the method. In comparison with the t0 sample, the stressed sample showed an increase in relative peak area for both HMWF and LMWF regions. The increased HMWF is likely due to the formation of aggregate, and the increased LMWF can result from the deconjugation of Fab under the elevated temperature. These results demonstrated that the SEC method is stability indicating.

Precision, Accuracy and Linearity

To assess the precision of the method, 18 injections of the conjugate sample were made using two HPLC instruments and two columns from different

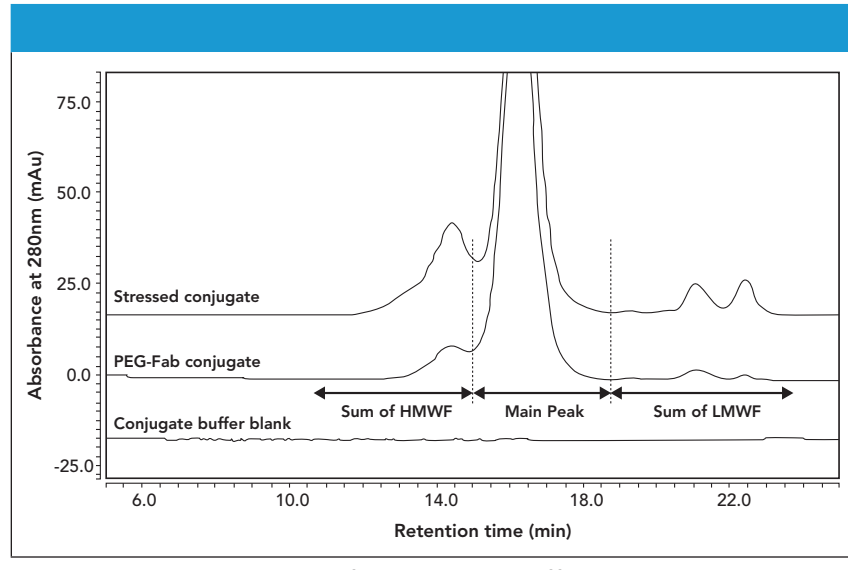

Figure 5: SEC chromatograms of the conjugate buffer blank, PEG–Fab conjugate (t0), and the stressed conjugate sample (4 weeks at 40 °C).

Table I: Test conditions for each parameter in the DOE study

Parameter	Test Conditions: Low (Center) High
Column temperature	26 (28) 30°C
Mobile phase [arginine]	270 (300) 330 mM
Mobile phase pH	6.1 (6.2) 6.3

lots. The %RSD of the relative peak area of the sum of HMWF, the main peak and the sum of LMWF is 1.2%, 0.1%, and 2.5%, respectively, demonstrates suitable precision.

For the linearity and accuracy assessment, five samples were prepared and injected at the concentrations of 2.5 mg/mL, 3.75 mg/mL, 5.0 mg/mL, 6.25 mg/mL and 7.5 mg/mL, corresponding to a range of 50% to 150% of the target protein loading (50 µg). The peak area of each region in the linearity samples was plotted against the theoretical protein loading and linear regression analysis was performed. The Pearson correlation coefficient (r) of the sum of HMWF, the main peak, and the sum of LMWF was 1.00 for each, and the percent recovery ranged from 100% to 114% at all loading levels. These results demonstrated a suitable linearity and accuracy of the method in the assessed range of 25 µg to 75 µg of protein loading.

Robustness by DOE

A DOE study was conducted to assess the method robustness by multivariate data analysis. Three parameters were identified as the potential significant sources of variation: column temperature, arginine concentration in the mobile phase, and the pH of the mobile phase. These parameters were evaluated in a full-factorial study design with eight test conditions and four replicates of the center point (Table I, Figure 6). Across all test conditions, the impact of each factor on the method performance was minimal. The resulted chromatograms overlaid well, and no significant changes in retention time and resolution between peaks of interest could be observed. The relative peak areas were further analyzed with a main effect plot (Figure 7). The parameters with the most significant impact on the quantitation were the level of arginine for the sum of HMWF and the column temperature for both the main peak and the sum of LMWF. However, the observed differences in the relative peak area were very close to the standard deviation of the center points; therefore, the SEC method was deemed robust for these tested parameters and no changes were made to the final SEC method.

Conclusion

In this study, we describe the development and optimization of a SEC method for monitoring of the size variants of a protein-polymer conjugate. Specific challenges related to the multimeric format of the conjugate, such as undesired secondary hydrophobic interactions with the column resin, were minimized with

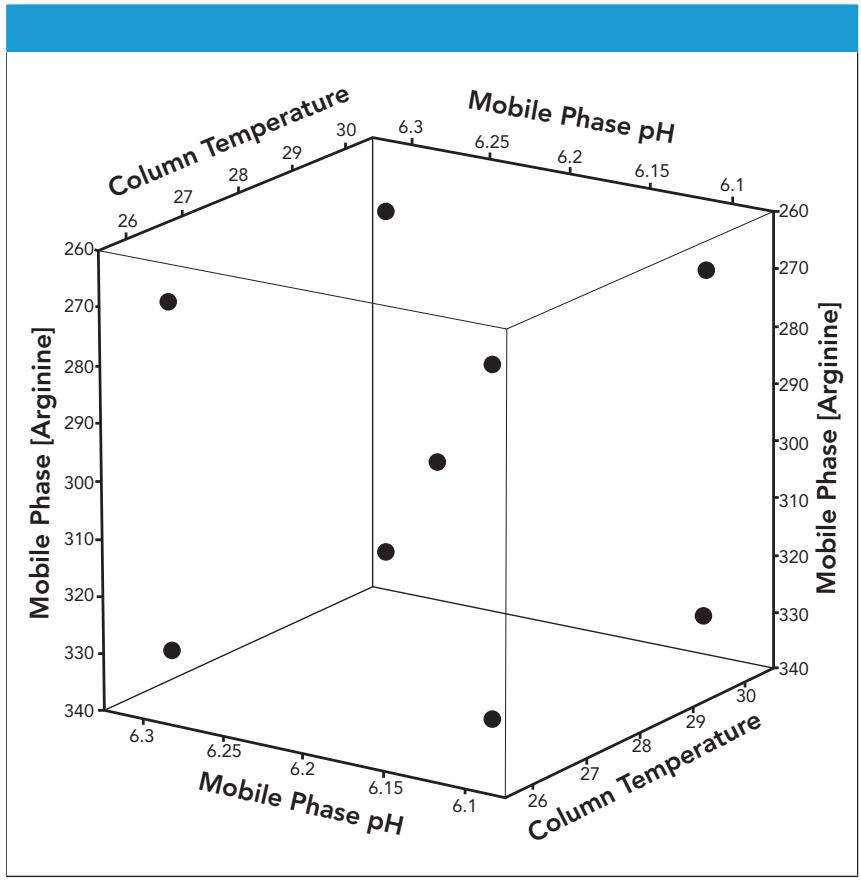

Figure 6: Cube plot showing the experimental conditions tested in the DOE study.

the final optimized method. The optimized method was further tested for specificity, precision, linearity, accuracy, stability indicating properties, and robustness. This study demonstrated that the SEC method is suitable for monitoring the size variants of the PEG–Fab conjugate and appropriate to support the manufacturing of clinical batches.

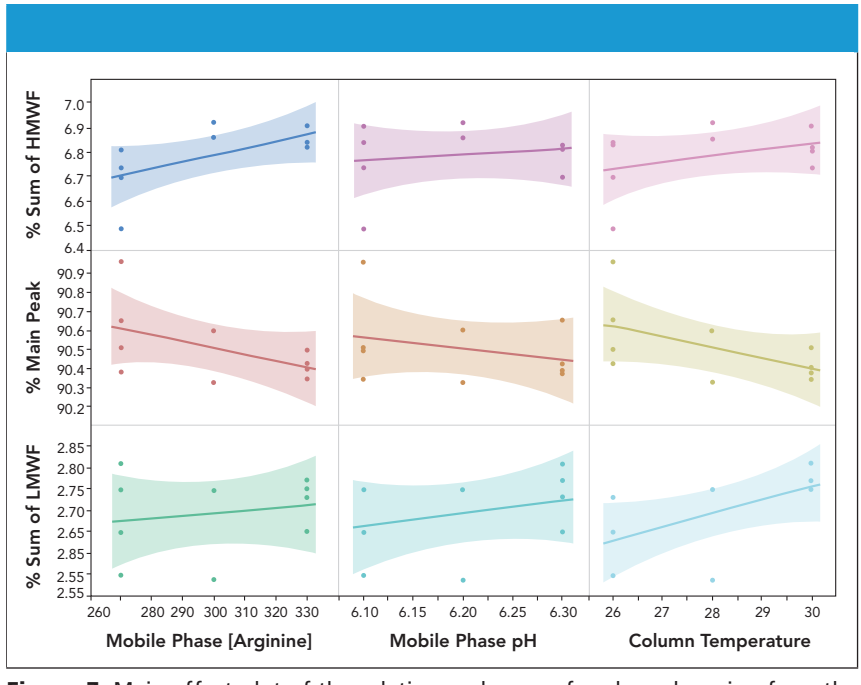

Figure 7: Main effect plot of the relative peak area of each peak region from the three-variable DOE study.

Acknowledgments

The authors would like to thank Tosoh Biosciences supplying the columns. Authors would also like to thank Dr. Aaron Wecksler and Dr. Matt Kalo from Genentech (South San Francisco, California) for providing critical review for this article, and Cinzia Stella for her guidance and support.

References

(1) J. M. Harris and R. B. Chess, *Nat. Rev. Drug Discov.* **2**(3), 214–221 (2003).

(2) F. M. Veronese and G. Pasut, *Drug Discovery Today* **10**(21), 1451–1458 (2005).

(3) H. Zhao, B. Rubio, P. Sapra, D. Wu, P. Reddy, P. Sai, A. Martinez, Y. Gao, Y. Lozanguiez, C. Longley, L.M. Greenberger, and I.D. Horak, *Bioconjugate Chem.* **19**(4), 849–859 (2008).

(4) A. Abuchowski, G.M. Kazo, C.R. Verhoest, Jr., T. Van Es, D. Kafkewitz, M.L. Nucci, A.T. Viau, and F.F. Davis, *Cancer Biochem. Biophys.* **7**(2), 175–186 (1984).

(5) R. B. Greenwald, Y. H. Choe, J. McGuire, and C. D. Conover, *Adv. Drug Deliv. Rev.* **55**(2), 217–250 (2003).

(6) W. Shatz, P.E. Hass, M. Mathieu, H.S. Kim, K. Leach, M. Zhou, Y. Crawford, A. Shen, K. Wang, D. P. Chang, M. Maia, S.R. Crowell, L. Dickmann, J.M. Scheer, and R.F. Kelley, *Mol. Pharmaceutics* **13**(9), 2996–3003 (2016).

(7) M. Swierczewska, K. C. Lee, and S. Lee, *Expert Opin. Emerg. Drugs* **20**(4), 531–536 (2015).

(8) W. Li, P. Zhan, E. De Clercq, H. Lou, and X. Liu, *Progress in Polymer Science* **38**(3–4), 421–444 (2013).

(9) T. Minko, *Drug Discov. Today Technol.* **2**(1), 15–20 (2005).

(10) W. Shatz, P.E. Hass, N. Peer, M.T. Paluch, C. Blanchette, G. Han, W. Sandoval, A. Morando, K.M. Loyet, V. Bantseev, H. Booler, S. Crowell, A. Kamath, J.M. Scheer, and R.F. Kelley, *PLOS ONE* **14**(6), e0218613 (2019).

(11) R. Yumioka, H. Sato, H. Tomizawa, Y. Yamasaki, and D. Ejima, *Journal of Pharmaceutical Sciences* **99**(2), 618–620 (2010).

Lu Dai and Fred Jacobson are with the Protein Analytical Chemistry group at Genentech, in South San Francisco, California. **Joseph Elich** worked at Genentech at the time the work was performed. Direct correspondence to: dai.lu@gene.com

CONNECT WITH LCGC ON SOCIAL MEDIA

Join your colleagues in conversation, respond to hot topic questions, and stay up-to-date on breaking news. "Like" and follow us on Twitter, LinkedIn, Facebook, and YouTube today!

LCGC

www.chromatographyonline.com/LCGCSocialMedia

SHIMADZU
Excellence in Science

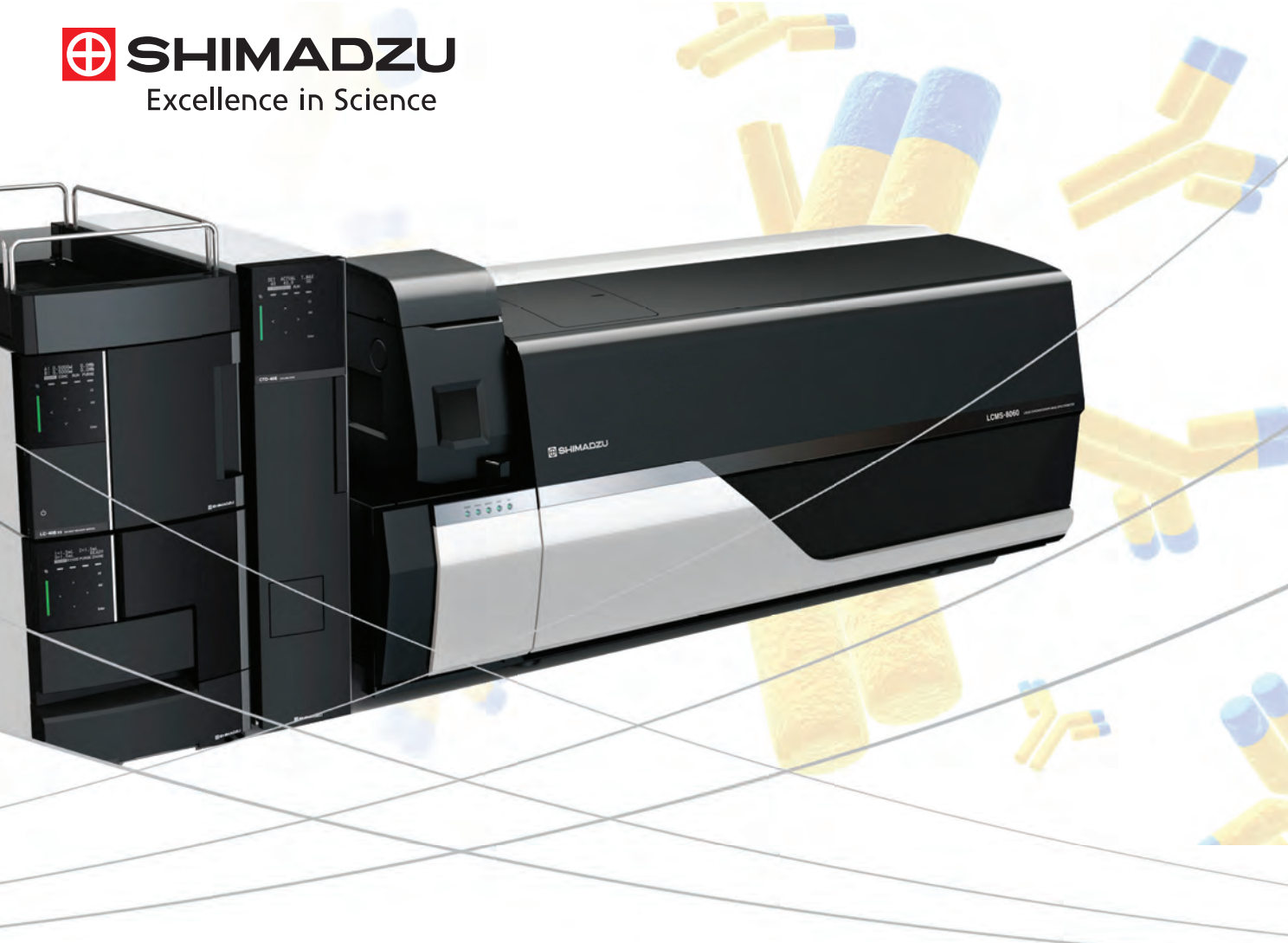

Accelerate your biopharma workflows with Shimadzu

At Shimadzu, we're focused on providing a total solution to biopharmaceutical workflows with an expansive portfolio of instrumentation that provides unparalleled performance. Utilize our precise, reliable platforms for research and discovery/development applications to clinical trials and quality management.

Key platforms include:

- ✓ Ultra-Fast & Sensitive LC-MS/MS for Quantitative Workflows
- ✓ LC-MS/MS Method Package for Cell Culture Media Profiling
- ✓ Compact Digital Ion Trap Mass Spectrometer
- ✓ Simplified Sample Prep Solution for Antibody Bioanalysis
- ✓ Ultra Fast Protein Digestion Platforms
- ✓ Ultra High Mass Analysis of Aggregates & Protein Complexes
- ✓ Truly Inert Platform for Bioseparations
- ✓ 2D HPLC for Analysis of Polysorbates
- ✓ Protein Sequencers

Learn more about Shimadzu's Biopharmaceutical solutions. Visit us online at

www.ssi.shimadzu.com

Shimadzu Scientific Instruments Inc., 7102 Riverwood Dr., Columbia, MD 21046, USA • (800) 477-1227